Susanne Nikolaus*, Markus Beu, Hans-Jörg Wittsack, Anja Müller-Lutz, Christina Antke, Hubertus Hautzel, Yuriko Mori, Eduards Mamlins, Gerald Antoch and Hans-Wilhelm Müller

GABAergic and glutamatergic effects on nigrostriatal and mesolimbic dopamine release in the rat

https://doi.org/10.1515/revneuro-2019-0112
Received December 2, 2019; accepted February 1, 2020; published online July 3, 2020

Abstract: In this review, a series of experiments is presented, in which γ-amino butyric acid (GABA)ergic and glutamatergic effects on dopamine function in the rat nigrostriatal and mesolimbic system was systematically assessed after pharmacological challenge with $GABA_A$ receptor (R) and and N-methyl D-aspartate (NMDA)R agonists and antagonists. In these studies, [^{123}I]iodobenzamide binding to the $D_{2/3}$R was mesured in nucleus accumbens (NAC), caudateputamen (CP), substantia nigra/ventral tegmental area (SN/VTA), frontal (FC), motor (MC) and parietal cortex (PC) as well as anterior (aHIPP) and posterior hippocampus (pHIPP) with small animal SPECT in baseline and after injection of either the $GABA_A$R agonist muscimol (1 mg/kg), the $GABA_A$R antagonist bicuculline (1 mg/kg), the NMDAR agonist D-cycloserine (20 mg/kg) or the NMDAR antagonist amantadine (40 mg/kg). Muscimol reduced $D_{2/3}$R binding in NAC, CP, SN/VTA, THAL and pHIPP, while, after amantadine, decreases were confined to NAC, CP and THAL. In contrast, D-cycloserine elevated $D_{2/3}$R binding in NAC, SN/VTA, THAL, frontal cortex, motor cortex, PC, aHIPP and pHIPP, while, after bicuculline, increases were confined to CP and THAL. Taken together, similar actions on regional dopamine levels were exterted by the $GABA_A$R agonist and the NMDAR antagonist on the one side and by the $GABA_A$R antagonist and the NMDAR agonist on the other, with agonistic action, however, affecting more brain regions. Thereby, network analysis suggests different roles of $GABA_A$Rs and NMDARs in the mediation of nigrostriatal, nigrothalamocortical and mesolimbocortical dopamine function.

Keywords: amantadine; bicuculline; $D_{2/3}$ receptor; D-cycloserine; $GABA_A$ receptor; muscimol; NMDA receptor; network analysis.

Introduction

The dopamin(DA)ergic system is under excitatory glutamat(GLU)ergic and inhibitory γ-amino butyric acid (GABA) ergic control (Figure 1). In the nigrostriatal system, the caudateputamen (CP) receives DAergic input from the pars compacta of the substantia nigra (SNc; Gerfen et al. 1987) and GLUergic input from neocortex and thalamus (THAL; Jayaraman 1985; Smeal et al. 2007). A further DAergic projection runs from the SNc to the neocortex, in particular to the frontal cortex (FC; Lindvall and Björklund 1974, 1978). The CP sends GABAergic efferents to the internal and the external part of the globus pallidus (GPi and GPe, respectively; Graybiel and Ragsdale 1979), and to the pars reticulata of the substantia nigra (SNr; Bolam et al. 1981). Via the direct pathway, GPi and SNr provide GABAergic input to the THAL (Albin et al. 1989). In the indirect pathway, the GPe sends GABAergic efferents to the subthalamic nucleus (STN), which, in turn, routes GLUergic fibers back to the GPe as well as to GPi and SNr (Carpenter et al. 1981; Albin et al. 1989). Further GABAergic projections run from CP and GP back to the SN (Hattori et al. 1975). Moreover, GLUergic fibers extend from THAL to neocortex (Kharazia and Weinberg 1994), from neocortex back to the THAL (Bromberg et al. 1981) and from either region back to the STN (Graybiel and Ragsdale 1979; Monakow et al. 1978).

In the mesolimbic system, the nucleus accumbens (NAC) receives DAergic input from ventral tegmental area (VTA; Lisman and Grace 2005), GLUergic input from THAL (Jayrayaman 1985), prefrontal cortex (PFC; Berendse et al.

Susanne Nikolaus and Markus Beu: These authors contributed equally to this article.

***Corresponding author: Susanne Nikolaus**, Clinic of Nuclear Medicine, University Hospital Düsseldorf, Moorenstr. 5, D-40225, Düsseldorf, Germany, E-mail: susanne.nikolaus@uni-duesseldorf.de. https://orcid.org/0000-0003-4899-3243
Markus Beu, Christina Antke, Yuriko Mori, Eduards Mamlins and Hans-Wilhelm Müller: Clinic of Nuclear Medicine, University Hospital Düsseldorf, Moorenstr. 5, D-40225, Düsseldorf, Germany
Hans-Jörg Wittsack, Anja Müller-Lutz and Gerald Antoch: Department of Diagnostic and Interventional Radiology, University Hospital Düsseldorf, Moorenstr. 5, D-40225, Düsseldorf, Germany
Hubertus Hautzel: Clinic for Nuclear Medicine, University Hospital Essen, Hufelandstraße 55, D-40225, Essen, Germany

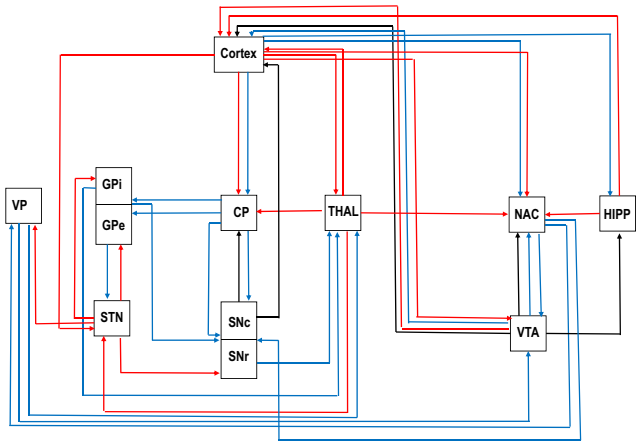

Figure 1: Diagram of relevant dopaminergic (black), GABAergic (blue) and glutamatergic connections (red) between substantia nigra (pars compacta [SNc], pars reticulata [SNr]), VTA, caudateputamen (CP), globus pallidus (internus [GPi], externus [GPe]), ventral pallidum (VP), nucleus subthalamicus (STN), nucleus accumbens (NAC), thalamus (THAL), hippocampus (HIPP) and neocortex.
The chart is based on the original reports given in the Introduction.

1992) and limbic regions including the HIPP (Walaas and Fonnum 1980a) as well as GABAergic input from VTA (Brown et al. 2012) and PFC (Lee et al. 2014). It sends GABAergic efferents back to the VTA (Walaas and Fonnum 1980b), to the SN (Walaas and Fonnum 1980b) and to the ventral pallidum (VP; Nauta and Cole 1978). The VP, in turn, receives GLUergic input from the STN (Turner et al. 2001) and provides GABAergic input to the THAL (Kuo and Carpenter 1973) and back to the VTA (Lisman and Grace 2005). Moreover, the VTA receives GLUergic input from the PFC (Carr and Sesack 2000) and sends DAergic efferents to neocortex (Lindvall and Björklund 1974, 1978) and HIPP (Gasbarri et al. 1991) as well as GABAergic efferents (Carr and Sesack 2000) to the neocortex. From the neocortex, GABAergic fibers run back to CP, NAC and limbic regions (Lee et al. 2014).

Dysfunctions of $GABA_A$ receptor (R), NMDAR and D_2R-like binding sites have been implied in a variety of neurological and neuropsychiatric disorders including Parkinson's disease, Huntington's disease, Alzheimer's disease, anxiety disorder, major depressive disorder and schizophrenia (for review see Nikolaus et al. 2009a,b, 2010, 2012, 2014a,b). Hence, it is of major importance to assess the functional relationships between DA and the GABAergic as well as GLUergic system. The present review, firstly, presents a series of small animal *in vivo* imaging studies, in which the interactions between DA and $GABA_AR$ as well as NMDAR function were systematically investigated in relevant regions of the nigrostriatal and mesolimbic system including NAC, CP, THAL, SN/VTA, FC, motor cortex (MC), parietal cortex (PC), anterodorsal HIPP (aHIPP) and posterior HIPP (pHIPP) using small animal SPECT and MRI (Nikolaus et al. 2017, 2018a,b, 2019a,b). For all of these regions, autoradiography studies have confirmed the presence of D_2R-like binding sites (Bouthennet et al. 1987, Seeman and Grigoriadis 1987, Morelli et al. 1990).

In our investigations, [^{123}I]S-3-iodo-N-(1-ethyl-2-pyrrolidinyl) methyl-2-hydroxy-6-methoxy benzamide ([^{123}I]IBZM) binding to the $D_{2/3}R$-subtype was measured in baseline and after pharmacological challenge with either muscimol (MUS; 5-aminomethyl-isoxazol-3-ol), bicuculline (BIC; (6R)-6-[(5 S)-6-methyl-5,6,7,8-tetrahydro[1,3]dioxolo[4,5-g]isoquinolin-5-yl] furo[3,4-e][1,3]benzodioxol-8(6H)-one)), D-cycloserine (DCS; D-4-amino-isoaxazolidinon) or amantadine (AMA; 1-amino-adamantane). Due to the competition between endogenous DA and the administered D_2R-like radioligand, this approach allows to gauge regional alterations of DA availability as induced by the respective pharmacological treatment in relation to baseline (for review see Laruelle 2000). In the present survey, the pool of regional $D_{2/3}R$ binding data was subjected to between-group comparisons, principal component analysis and network analysis in order to assess the specific impact of the individual challenges on regional DA function and DAergic interactions between regions.

Study 1: $D_{2/3}R$ binding after $GABA_AR$ agonistic treatment

Aim

MUS is as highly selective $GABA_AR$ agonist (inhibition constant [K_i] = 2.7 nM; Negro et al. 1995). We had previously shown that D_2R-like imaging can be employed in order to estimate alterations of synaptic DA upon challenge with compounds such as methylphenidate and L-DOPA, which modify DA availability in the synaptic cleft (for review see Nikolaus et al. 2011). So far, effects of MUS on cerebral DA concentrations had not been assessed using *in vivo* small animal imaging methods. Therefore, in our first *in vivo* imaging study of DA and GABA interaction we set out to determine the effect of MUS on nigrostriatal and mesolimbic $D_{2/3}R$-like binding (Nikolaus et al. 2017, 2018a,b).

Methods

Fifteen adult male Wistar rats (ZETT, Heinrich-Heine University, Düsseldorf, Germany; weight: 439 ± 23 g [mean ± standard deviation {SD}]) underwent SPECT measurements in baseline (no pre-treatment) and after

challenge with MUS (Sigma-Aldrich, Taufkirchen, Germany; dose: 1 mg/kg). The dose of 1 mg/kg had been previously shown to be behaviorally active at 10 to 30 min after systemic application (e. g., Corbett et al. 1991, Oakley et al. 1991). Hence, at 30 min post-challenge, animals were injected [^{123}I]IBZM (GE Healthcare, München, Germany; mean activity in baseline and post-challenge: 26 ± 4 MBq) into the lateral tail vein. [^{123}I]IBZM exhibits a high affinity for the D_2R-like subtype (D_2: K_i = 1.6 nM, D_3: K_i = 2.2 nM; Videbaek et al. 2000). Furthermore, the benzamide analogue [^{11}C] raclopride displays similar affinities for the high- and low-affinity state of the D_2R-like subtype (Seneca et al. 2006), which implies that also [^{123}I]IBZM binds to D_2R-like binding sites in both configurations and that the regional binding potentials (BPs) obtained in the present studies reflect the regional densities of $D_{2/3}$Rs as such, irrespective of the individual contributions of either affinity state.

In our series of studies, we employed a two-modality imaging approach, in which regional volumes of interest (VOIs) were defined on overlays of functional SPECT and morphological MRI data sets. $D_{2/3}$R binding data were acquired with the "TierSPECT" (field of view: 90 mm; spatial resolution: 3.4 mm for ^{123}I; Schramm et al. 2000) from 45 to 105 min after radioligand administration, corresponding to 75–135 min post-challenge and coinciding with the time of maximum striatal DA levels (75 to 195 min min post-challenge) upon MUS administration (Santiago and Westerink. 1992). Radioligand administration and SPECT measurements were performed in animals anaesthetized with ketaminehydrochloride (Ketavet®, Pharmacia GmbH, Erlangen, Germany; dose: 100 mg/kg) and xylazinehydrochloride (Rompun® Bayer, Leverkusen, Germany; dose: 5 mg/kg i.p.). Morphological images of the rat heads were obtained with a dedicated small animal MRI (MRS3000 Pre-clinical MRI, 3.0 T, MR Solutions, Guildford, UK; coil diameter: 54 mm, acquisition time: 553 s, spatial resolution: 0.25 × 9.25 × 0.69 mm).

Findings

Figure 2A shows characteristic coronal images of regional [^{123}I]IBZM accumulations in baseline and after challenge with MUS at different positions from Bregma (Paxinos and Watson 2014) obtained in the same rat.

MUS significantly (non-parametric Wilcoxon signed rank test for paired samples, two-tailed, $\alpha \leq 0.05$) reduced $D_{2/3}$R BPs in NAC (median: 74% of baseline, 25-percentile: 52%, 75-percentile: 99%), CP (median: 82% of baseline, 25-percentile: 74%, 75-percentile: 92%), SN/VTA (median: 74% of baseline, 25-percentile: 54%, 75-percentile: 84%), THAL (median: 81% of baseline, 25-percentile: 62%, 75-percentile: 102%) and pHIPP (median: 77% of baseline, 25-percentile: 68%, 75-percentile: 100%; Figure 4).

Previous *in vivo* microdialysis studies have shown that MUS infusions (0.1–40 µM) into the PFC (Matsumoto et al. 2003) and into the VTA (Westerink et al. 1996, 1998) reduced DA concentrations in CP (Matsumoto et al. 2003; Westerink et al. 1996) and PFC (Westerink et al. 1998). In contrast, however, MUS infusions (10–100 µM) into SN (Santiago and Westerink 1992) and GP (Cobb and Abercrombie 2002, 2003) augmented DA concentrations in CP and SN, respectively. Regional alterations of DA availability are commonly assessed *in vivo* by two measurements of D_2R-like binding – once before and once after the administration of compounds, which augment DA concentration in the synaptic cleft (for review see Laruelle 2000). The principle underlying this approach is the competition between endogenous DA and the administered D_2R-like radioligand. Thus, our finding of reduced $D_{2/3}$R binding in NAC, CP, SN/VTA, THAL and pHIPP can be interpreted to reflect increased availability of DA in these regions, which is in agreement with the precedent findings of elevated DA levels in CP (Santiago and Westerink 1992) and SN (Cobb and Abercrombie 2002, 2003) upon administration of MUS into SN and GP, respectively. Interestingly, however, our results after systemic treatment as well as the findings obtained after infusion into SN (Santiago and Westerink 1992) and GP (Cobb and Abercrombie 2002, 2003) contradict the reports of Westerink et al. (1996, 1998) and Matsumoto et al. (2003), who found reductions of striatal and prefrontal DA levels upon administration of MUS into PFC and VTA, respectively. This inconsistency highlights the region-specificy of intracerebral MUS action.

Study 2: $D_{2/3}$R binding after $GABA_A$R antagonistic treatment

Aim

BIC is a highly selective $GABA_A$R antagonist (K_i = 3.04 nM; Ito et al. 1988). So far, effects of BIC on cerebral DA concentrations had not been assessed using *in vivo* small animal imaging methods. Hence, in our second study, we set out to

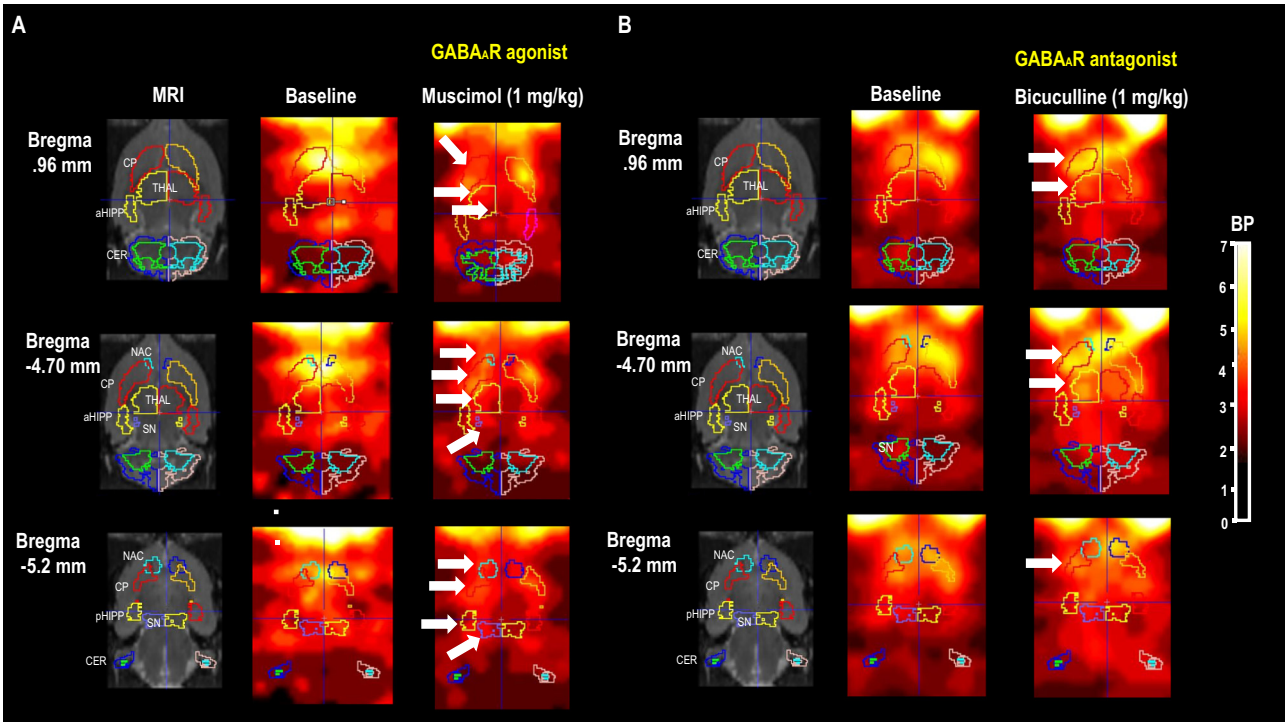

Figure 2: [^{123}I]IBZM binding to $D_{2/3}$R in baseline and after challenge with the $GABA_AR$ agonist muscimol (1 mg/kg i.p.) and the $GABA_AR$ antagonist bicuculline (1 mg/kg i.p.) at different positions from Bregma (Paxinos and Watson, 2014).
The white arrows indicate the significant reductions after challenge relative to baseline. All images show BPs (ratios of specific binding to non-specific binding in the cerebellum [CER]). Data were evaluated with PMOD (version 3.5, PMOD Technologies Ltd., Zürich, Switzerland). Regional VOIs (NAC, CP, SN/VTA, THAL, FC. MC. PC, aHIPP, pHIPP) were defined on overlays of SPECT images of [^{123}I]IBZM binding (formerly coregistered with MRI) with the standard Paxinos rat brain MRI (Schiffer et al., 2006). Abbreviations: NAC, nucleus accumbens; CP, caudateputamen; SN, substantia nigra/ventral tegmental area; THAL, thalamus; FC, frontal cortex; MC, motor cortex; PC, parietal cortex; aHIPP, anteriodorsal hippocamus; pHIPP, posterior hippocampus; CER, cerebellum; BP, binding potential.

determine the effect of BIC on nigrostriatal and mesolimbic $D_{2/3}$R-like binding (Nikolaus et al. 2017, 2018a).

Methods

Sixteen adult male Wistar rats (weight: 433 ± 28 g) underwent SPECT measurements in baseline and after challenge with BIC (Sigma-Aldrich, Taufkirchen, Germany; dose: 1 mg/kg). This dose had been previously shown to be subconvulsant (Girardi et al. 1987), but behaviorally active after systemic application (Zhang and Cranney 2008). Therefore, at 30 min post-challenge, animals were injected [^{123}I]IBZM (mean activity in baseline and post-challenge: 26 ± 5 MBq) into the lateral tail vein. Again, $D_{2/3}$R binding data were acquired with the "TierSPECT" (see above) from 45 to 105 min after radioligand administration), corresponding to 75–135 min post-challenge and coinciding with the time of maximum striatal DA levels (75–195 min min post-challenge) upon administration of BIC (Santiago and Westerink. 1992).

Findings

Figure 2B shows characteristic coronal images of regional [^{123}I]IBZM accumulations in baseline and after challenge with BIC at different positions from Bregma (Paxinos and Watson 2014) obtained in the same rat.

BIC significantly (non-parametric Wilcoxon signed rank test for paired samples, two-tailed, $\alpha \leq 0.05$) elevated BPs in CP (median: 112% of baseline, 25-percentile: 98%, 75-percentile: 121%) and THAL (median: 116% of baseline, 25-percentile: 98%, 75-percentile: 131%; Figure 4).

Previous *in vivo* microdialysis studies have shown that BIC infusions (20–100 µM) into SN (Santiago and Westerink 1992; Westerink et al. 1992), VTA (Ikemoto et al. 1997) and PFC (Karreman and Moghaddam 1996; Matsumoto et al. 2003) increased DA levels in SN and CP (Santiago and Westerink 1992; Westerink et al. 1992) as well as NAC (Ikemoto et al. 1997) and PFC (Karreman and Moghaddam 1996; Matsumoto et al. 2003). Thus, if the data obtained in the present study after BIC are interpreted to reflect

reductions of endogenous DA, the obtained findings do not agree with the precedent *in vivo* microdialysis studies. This inconsistency, may be accounted for by differences in applied doses (2.7 mM in our study vs 10–100 µM [Aono et al. 2008; Ikemoto et al. 1997; Karreman and Moghaddam 1996; Matsumoto et al. 2003; Santiago and Westerink 1992; Smolders et al. 1995; Westerink et al. 1992; Yan et al. 1999]) and mode of application (systemic approach vs intracerebral injection).

Study 3: $D_{2/3}$R binding after NMDAR agonistic treatment

Aim

DCS is an NMDAR agonist, which binds with high affinity to the $glycine_B$ NMDAR subunit (K_i = 2.33; Monahan et al. 1989). So far, effects of DCS on cerebral DA concentrations had not been assessed using *in vivo* small animal imaging methods. In our next study (Nikolaus et al. 2019a) we set out to determine the effect of DCS on nigrostriatal and mesolimbic $D_{2/3}$R-like binding.

Methods

Fifteen adult male Wistar rats (weight: 374 ± 40 g) underwent SPECT measurements in baseline and after challenge with DCS (Sigma-Aldrich, Taufkirchen, Germany; dose: 20 mg/kg). This dose had been previously shown to be behaviorally active after systemic application (Zlomuzica et al. 2007). At 30 min post-challenge, animals were injected [^{123}I]IBZM (mean activity in baseline and post-challenge: 28 ± 4 MBq) into the lateral tail vein. $D_{2/3}$R binding data were acquired with the "TierSPECT" (see above) from 45 to 105 min after radioligand administration, corresponding to 75 to 135 min post-challenge and coinciding with the time of maximum striatal DA levels (80 to 160 min min post-challenge after administration of DCS (Gandolfi et al. 1994).

Findings

Figure 3A shows characteristic coronal images of regional [^{123}I]IBZM accumulations in baseline and after challenge with DCS at different positions from Bregma (Paxinos and Watson 2014) obtained in the same rat.

DCS significantly (non-parametric Wilcoxon signed rank test for paired samples, two-tailed, $\alpha \leq 0.05$) elevated BPs in NAC (median: 112% of baseline, 25-percentile: 104%, 75-percentile: 127%), SN/VTA (median: 127% of baseline, 25-percentile: 104%, 75-percentile: 152%), THAL (median: 116% of baseline, 25-percentile: 93%, 75-percentile: 135%), MC (median: 119% of baseline, 25-percentile: 104%, 75-percentile: 152%), PC (median: 110% of baseline, 25-percentile: 101%, 75-percentile: 142%), aHIPP (median: 119% of baseline, 25-percentile: 97%, 75-percentile: 150%) and pHIPP (median: 127% of baseline, 25-percentile: 93%, 75-percentile: 153%; Figure 4).

So far, the effect of systemic DCS (3 and 30 mg/kg) had only been assessed in the rat CP, where either a significant elevation (Bennett and Gronier 2005) or no effect (Gandolfi et al. 1994) on DA efflux was observed. The former contradicts our findings, which did not show an alteration of $D_{2/3}$R binding in the CP after 20 mg/kg DCS. Likely reasons for this inconsistency are the differences in methods (*in vivo* SPECT in our study vs assessment of striatal homogenates with high pressure liquid chromatography), mode of application (systemic approach *vs* incubation of striatal slices) and age of subjects (adult rats with a mean weight of 397 ± 49 g in our study *vs* adolesent animals, weighing between 250 and 350 g).

Study 4: $D_{2/3}$R binding after NMDAR antagonistic treatment

Aim

The NMDAR antagonistic AMA binds to the phencyclidine NMDAR binding site (K_i = 10 µM; Kornhuber et al. 1991, 1993). After chronic treatment with AMA (200 mg/day for at least 10 days), two *in vivo* imaging studies of striatal D_2R-like binding have been conducted on Parkinsonian patients with [^{11}C]raclopride as radioligand (Moresco et al. 2002; Volonte et al. 2001). In both investigations, striatal D_2R-like binding was significantly elevated, implying that, at least in individuals suffering from Parkinson's disease, the AMA-induced elevation of endogenous DA was not high enough to elicit a detecable competition with the exogenous radioligand. Therefore, in our next study (Nikolaus et al. 2019a,b) we set out to determine the effect of AMA on nigrostriatal and mesolimbic $D_{2/3}$R-like binding in healthy rats, which–contrasting with the human subjects of Volonte et al. (2001) as well es Moreso et al. (2002) - had not been inflicted Parkinsonian lesions.

Methods

Twenty adult male Wistar rats (weight: 414 ± 48 g) underwent SPECT measurements in baseline and after challenge with AMA (Sigma-Aldrich, Taufkirchen, Germany; dose: 40 mg/kg). The 40 mg/kg dose had formerly been shown to be behaviorally active in rats after systemic application (Maj et al. 1972). At 30 min post-challenge, animals were injected [^{123}I]IBZM (mean activity in baseline and post-challenge: 28 ± 4 MBq) into the lateral tail vein. $D_{2/3}$R binding data were acquired with the "TierSPECT" (see above) from 45 to 105 min after radioligand administration, corresponding to 75–135 min post-challenge and coinciding with the time of maximum striatal DA levels (60 to 90 min post-challenge) after administration of AMA (Takahashi et al. 1996).

Findings

Figure 3B shows characteristic coronal images of regional [^{123}I]IBZM accumulations in baseline and after challenge with AMA at different positions from Bregma (Paxinos and Watson 2014) obtained in the same rat.

AMA significantly (non-parametric Wilcoxon signed rank test for paired samples, two-tailed, $\alpha \leq 0.05$) diminished BPs in NAC (median: 90% of baseline, 25-percentile: 70%, 75-percentile: 101%), CP (median: 82% of baseline, 25-percentile: 72%, 75-percentile: 106%) and THAL (median: 79% of baseline, 25-percentile: 71%, 75-percentile: 106%; Figure 4).

So far, the effect of systemic AMA on DA had only been assessed in the CP. The present finding of elevated DA in this region is consistent with the results obtained in various studies after AMA doses between 40 and 100 mg/kg i.p. or s.c. (Scatton et al. 1970, Quack et al. 1995, Takahashi et al. 1996). They are not in agreement, however, with the findings of Maj et al. (1972) as well as Bak et al. (*1972*), who did not observe changes in striatal DA after 10 to 100 mg/kg AMA i.p. Again, this may be accounted for by differences in methods: the precedent investigations either employed invasive *in vivo* methods such as microdialysis (Quack et al. 1995, Takahashi et al. 1996) or *ex vivo* methods involving the preparation of striatal tissue extracts (Bak et al. 1972, Maj et al. 1972, Scatton et al. 1970). Scatton et al. (1970), who found an increase of striatal DA, sacrificed their rats 2 h post-challenge, whereas Bak et al. (1972) as well as Maj et al. (1972), who observed no significant effects, killed their animals only 1 h post-challenge. Thus, it may be concluded that a time of 1 h post-challenge is not sufficient to detect changes in DA levels, if combined with *ex vivo* methods, precluding AMA action to take place in living compartments.

Comparisons of regional $D_{2/3}$R binding between treatments

Regional $D_{2/3}$R binding ($D_{2/3}$R BP after challenge expressed as percentage of baseline) was compared between treatment groups (MUS, BIC, DCS, AMA). Since in neither treatment group data were uniformly normally distributed (Kolmogorov-Smirnov test, $0001 \leq p \leq .20$), groups were compared with non-parametric Kruskal-Wallis analysis of variance (two-tailed, $\alpha \leq 0.05$) and Mann-Whitney U tests (two-tailed, $\alpha \leq 0.05$). No corrections were made for multiple comparisons. Tests were performed with IBM SPSS Statistics 23 (IBM SPSS Software Germany, Ehningen, Germany).

Figure 3 shows the regional $D_{2/3}$R BPs after challenge with MUS, BIC, DCS and AMA expressed as percentages of baseline. The Kruskal-Wallis test yielded significant differences of BP percentages of baseline between treatment groups in all brain regions (NAC: $p \leq 0.0001$, CP: $p = 0.001$, SN/VTA: $p \leq 0.0001$, THAL: $p = 0.001$, FC: $p = 0.052$, MC: $p = 0.004$, PC: $p = 0.001$, aHIPP: $p = 0.010$, pHIPP: $p = 0.009$). Individual comparisons between treatment groups with the Mann-Whitney *U* test yielded (1) significant decreases of BP percentages of baseline after MUS relative to BIC in NAC ($p = 0.037$), CP ($p = 0.004$), SN/VTA ($p = 0.001$), THAL ($p = 0.006$), PC ($p = 0.044$) and aHIPP ($p = 0.044$); (2) significant decreases of BP percentages of baseline after MUS relative to DCS in NAC (≤ 0.0001), CP ($p \leq 0.0001$), SN/VTA ($p \leq 0.0001$), THAL ($p = 0.004$), FC ($p = 0.026$), MC ($p = 0.010$), PC ($p \leq 0.0001$), aHIPP ($p = 0.002$) and pHIPP ($p = 0.003$); (3) significant decreases of BP percentages of baseline after MUS relative to AMA in SN/VTA ($p = 0.047$) and PC ($p = 0.037$); (4) significant decreases of BP percentages of baseline after BIC relative to DCS in PC ($p = 0.013$); (5) significant decreases of BP ratios after BIC relative to AMA in NAC ($p = 0.013$), CP ($p = 0.017$), THAL ($p = 0.002$) and MC ($p = 0.050$); (6) significant decreases of BP percentages of baseline after DCS relative to AMA in NAC ($p \leq 0.0001$), CP ($p = 0.012$), SN/VTA ($p = 0.017$), THAL ($p = 0.003$), FC ($p = 0.045$), MC ($p = 0.001$), PC ($p = 0.025$), aHIPP ($p = 0.012$) and pHIPP ($p = 0.009$).

Principal component analysis

Using an orthogonal transformation, principal component analysis converts a set of possibly correlated variables (in the present analysis: BP percentages relative to baseline in NAC, CP, SN/VTA, THAL, FC, MC, PC, aHIPP and pHIPP

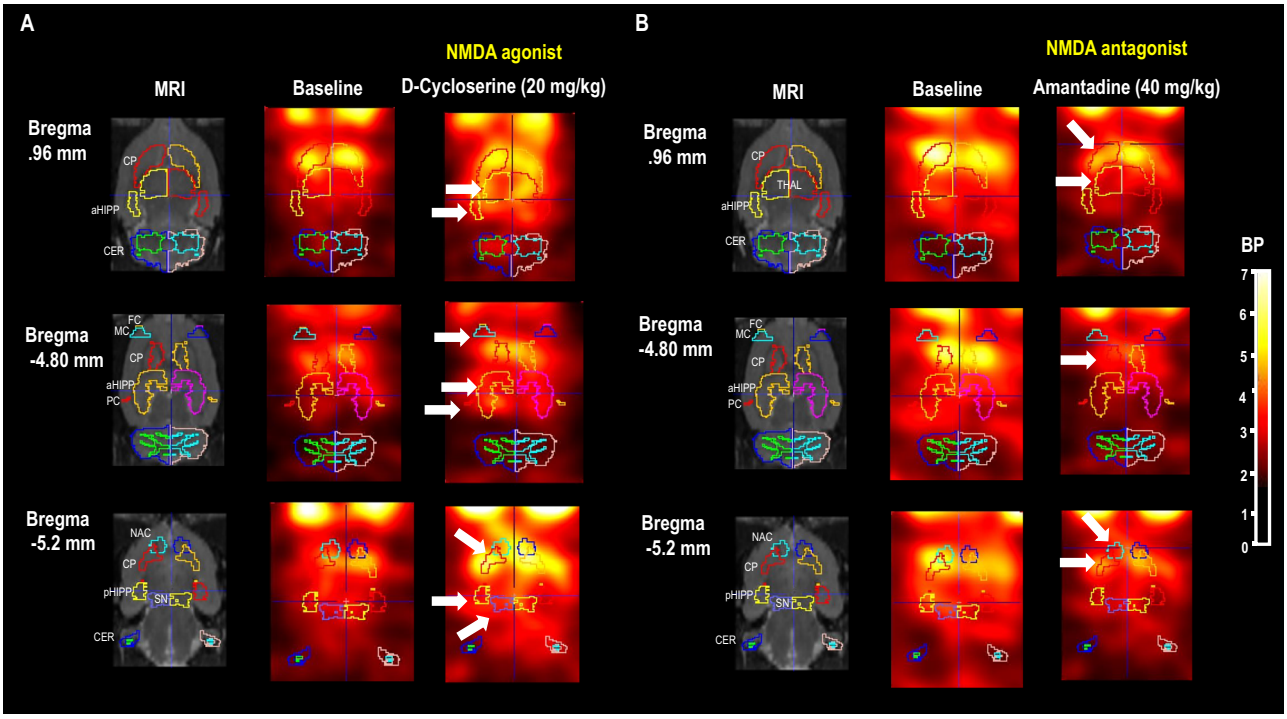

Figure 3: [^{123}I]IBZM binding to $D_{2/3}R$ in baseline and after challenge with the NMDAR agonist D-cycloserine (20 mg/kg i.p.) and the NMDAR antagonist amantadine (40 mg/kg i.p.) at different positions from Bregma (Paxinos and Watson, 2014).
The white arrows indicate the significant reductions after challenge relative to baseline. All images show BPs (ratios of specific binding to non-specific binding in the cerebellum [CER]). Data were evaluated with PMOD (version 3.5, PMOD Technologies Ltd., Zürich, Switzerland). Regional VOIs (NAC, CP, SN/VTA, THAL, FC. MC. PC, aHIPP, pHIPP) were defined on overlays of SPECT images of [^{123}I]IBZM binding (formerly coregistered with MRI) with the standard Paxinos rat brain MRI (Schiffer et al., 2006). Abbreviations: NAC, nucleus accumbens; CP, caudateputamen; SN, substantia nigra/ventral tegmental area; THAL, thalamus; FC, frontal cortex; MC, motor cortex; PC, parietal cortex; aHIPP, anteriodorsal hippocamus; pHIPP, posterior hippocampus; CER, cerebellum; BP, binding potential.

with all treatments pooled) into a set of linearly uncorrelated variables, the so-called principal components. In the resulting new coordinate system, the greatest (second greatest, third greatest etc.) variance of the data lies on the first (second, third etc.) coordinate, yielding the first (second, third etc.) PrC, which, thus, accounts for the greatest (second greatest, third greatest etc.) variability in the data set. Here, the principal component analysis was performed according to Hotelling (1933), yielding eigenvalues (the PrCs) and the eigenvector components contributing to the individual principal components. The principal component analysis was performed using Rapid Miner (version 5.3., Rapid-I GmbH, Dortmund, Germany).

Principal component analyis revealed that 56% of the cumulative variance of the whole data set ($D_{2/3}R$ BPs expressed as percentage of baseline with all treatments pooled) could be explained by the first principal component (PrC1), while PrC2 to PrC9 added up to 72.9, 80.7, 85.6, 90.1, 94.2, 96.7%, 98,8 and 100%, respectively, of the cumulative variance (Table 1). The eigenvector component with the highest contribution (38.4%) to PrC1 was the $D_{2/3}R$ BP (expressed as percentage of baseline) in the CP. The major eigenvector components of the other principal components were the BP percentages of baseline in SN/VTA (43.2%, PrC2 and 54.2%, PrC6), FC (39.7%, PrC3), THAL (41.3%, PrC4), PC (75.6%, PrC5), MC (50%, PrC7 and 49.7%, PrC8) and NAC (58.5%, PrC9).

Network analysis

Network analysis permits to analyse the network structure of variables - pre-defined so-called “nodes” - by estimating path coefficients, which describe the “strength” of the individual connections. Here, we assessed the associations between $D_{2/3}R$ binding in the individual brain regions (CP, NAC, THAL, SN/VTA, FC, MC, PC, aHIPP and pHIPP), based (1) on the regional $D_{2/3}R$ BPs in baseline with all four treatments groups pooled, (2) on the regional $D_{2/3}R$ BPs (expressed as percentage of baseline) obtained after the individual challenges with MUS, AMA, DCS and BIC, and, (3) on the regional $D_{2/3}R$ BPs (expressed as percentage of

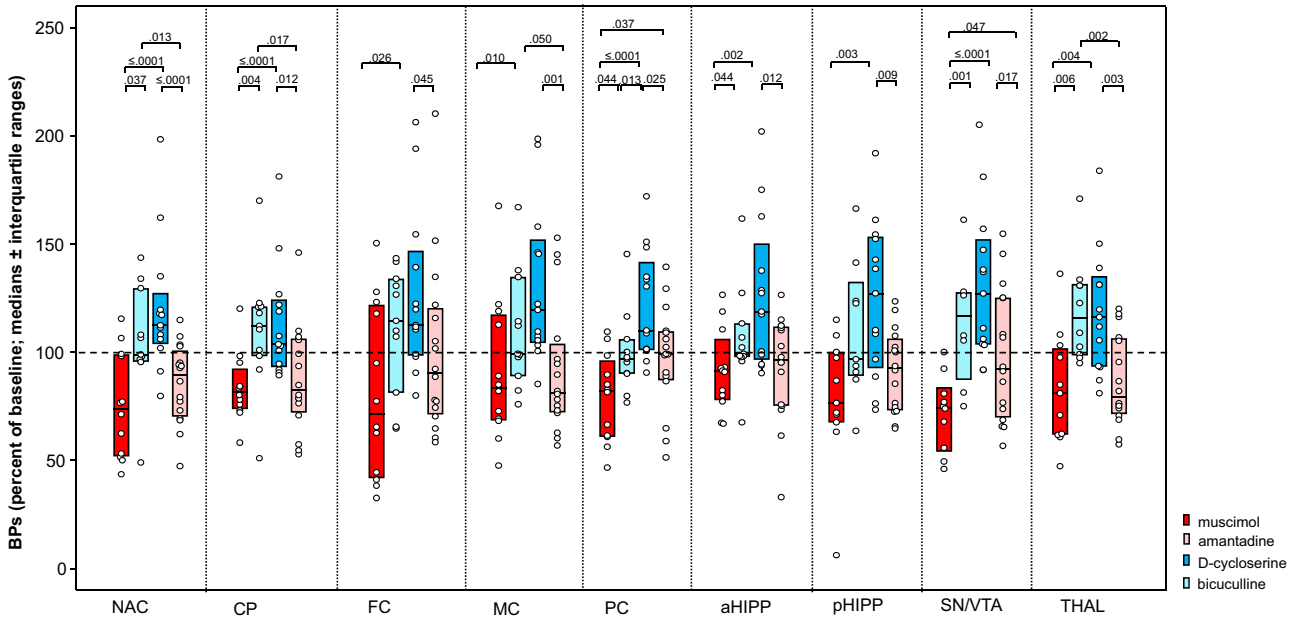

Figure 4: Binding potentials (BPs; expressed as ratios to baseline) after challenge with 1 mg/kg muscimol (red), 40 mg/kg amantadine (pink), 1 mg/kg bicuculline (blue) and 20 mg/kg D-cycloserine (light blue).
Estimations of regional $D_{2/3}R$ binding potentials (BPs) for baseline and challenges were obtained according to the simplified reference tissue model (Ichise et al., 2001) by computing ratios of radioactvity counts obtained in the specifically-bound compartments (nucleus accumbens [NAC], caudateputamen [CP], thalamus [THAL], substantia nigra/ventral tegmental area [SN/VTA], frontal cortex [FC], motor cortex [MC], parietal cortex [PC], anterodorsal hippocampus [aHIPP], posterior hippocampus [pHIPP]) to radioactivity counts in the cerebellum (CER). Rendered are medians and 25-/75-percetiles (boxes). The circles represent the individual animals. For significant between-group differences, the respective p values are given (Wilcoxon Mann Whitney *U* test for unrelated samples, two-tailed, $\alpha = .05$). Calculations were performed with IBM SPSS Statistics 23 (IBM SPSS Software Germany, Ehningen, Germany).

baseline) with either $GABA_AR$ agonistic (MUS) and NMDAR antagonistic (AMA) or $GABA_AR$ antagonistc (BIC) and NMDAR agonistic (DCS) challenges pooled. Covariance matrices were estimated with pairwise Mixed Graphical Models (MGMs; Haslbeck and Waldorp 2015, Yang et al. 2014). Graphical L_1 (lasso) regularized regression was employed in order to increase matrix sparsity (Friedman et al. 2008). In baseline and after each treatment, missing binding data were replaced by the respective average BP. MGMs were computed using JASP (version 0.10.2.0, JASP Team 2019, ©2013-2019 University of Amsterdam).

Table 1: Main results of principal component analysis.

PrCs	% of VAR accounted for by PrCs	Regional eigenvectors with the highest contribution to PrCs	% of VAR accounted for by the eigenvectors with the highest contribution to PrCs
PrC1	56.0	CP	38.4
PrC2	17.0	SN/VTA	43.2
PrC3	7.8	FC	39.7
PrC4	4.9	THAL	41.3
PrC5	4.5	PC	76.0
PrC6	4.1	SN/VTA	54.2
PrC7	2.5	MC	50.0
PrC8	2.0	MC	49.7
PrC9	1.2	NAC	58.5

PrC, principal component; VAR, variance.

Network analysis of baseline BPs yielded 14 out of 36 possible connections (Figure 5A; sparsity: 0.611). Table 2 shows the individual path coeffients (c) with the strongest associations between CP and NAC (c = 0.566), FC and MC (c = 0.414), CP and THAL (c = 0.366), THAL and aHIPP (c = 0.348), SN/VTA and pHIPP (c = 0.330), MC and aHIPP (c = 0.242) and MC and PC (c = 0.211).

When the regional $D_{2/3}R$ BPs obtained after the individual challenges were subjected to network analysis, five out of 36 (sparsity: 0.861) and nine out of 36 possible connections (sparsity: 0.750) were obtained for MUS and AMA, respectively. Moreover, network analysis yielded four out of 36 (sparsity: 0.0889) and three out of 36 possible connections (sparsity: 0.917) for BIC and DCS, respectively (Figure 5B, Table 3). After treatment with the $GABA_AR$ agonistic MUS, the strongest associations were found between MC and PC (c = 0.971), CP and THAL (c = 0.459) and SN/VTA and pHIPP (c = 0.314). Treatment with the $GABA_AR$

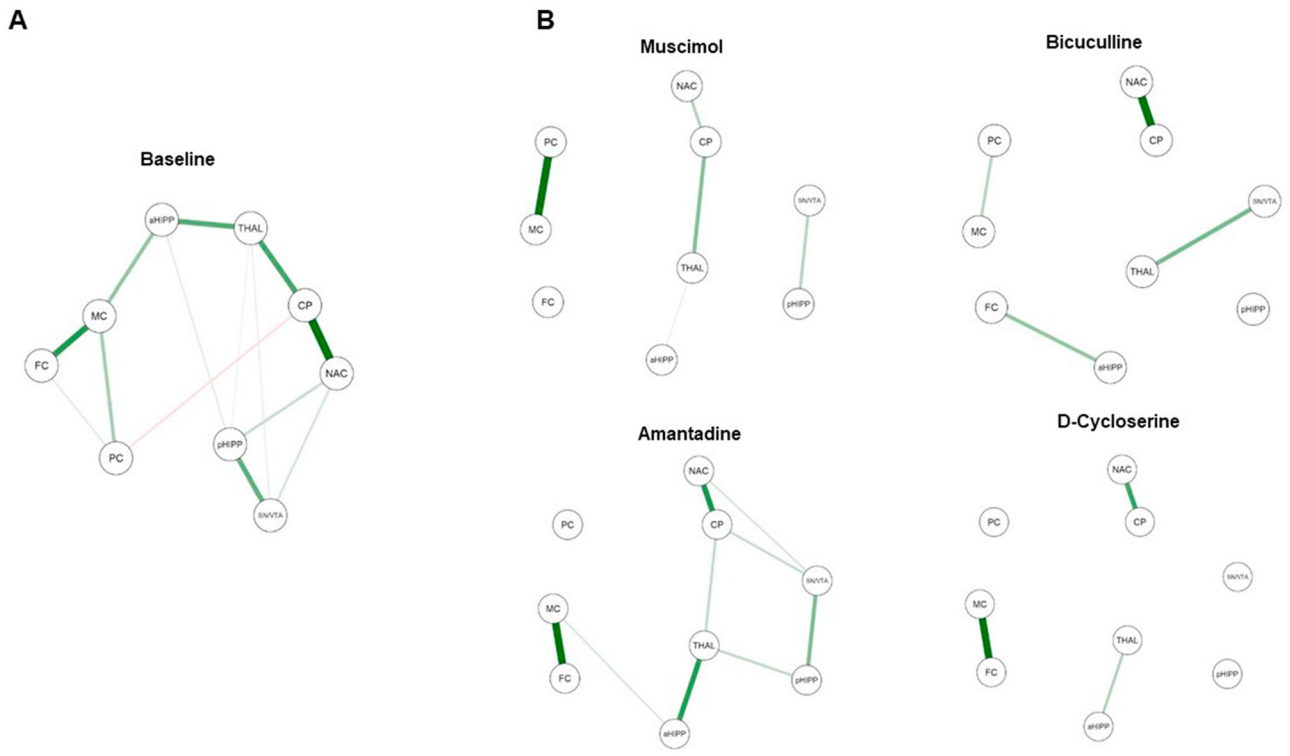

Figure 5: Connections between nucleus accumbes (NAC), caudeputamen (CP), thalamus (THAL), substantia nigra/ventral tegmental area (SN/VTA), frontal cortex (FC), motor cortex (MC), parietal cortex (PC), anterodorsal hippocampus (aHIPP) and posterior hippocampus (pHIPP). (A) Connections obtained in baseline. (B) Connections obtained after the individual challenges with muscimol, bicuculline, amantadine or D-cycloserine. Positive and negative association are represented by green and red lines, respectively. The size of the lines indicates the strength of the individual connections. Models were estimated with JASP (version 0.10.2.0, JASP Team, 2019, ©2013–2019 University of Amsterdam).

antagonistic BIC yielded the strongest associations between CP and NAC (c = 0.744), SN/VTA and THAL (c = 0.386), FC and aHIPP (c = 0.321) and MC and PC (c = 0.235). After treatment with the NMDAR agonistic DCS, the strongest associations were found between FC and MC and CP and NAC (c = 0.595, each). After the NMDAR antagonistic AMA, the strongest associations existed between FC and MC (c = 0.626), CP and NAC (c = 0.472), THAL and aHIPP (c = 0.445) and SN/VTA and pHIPP (c = 0.311).

When regional $D_{2/3}R$ BPs were subjected to network analysis with either $GABA_AR$ agonistic and NMDAR

Table 2: Path coefficient matrix in baseline obtained with mixed graphical modelling of all $D_{2/3}R$ binding potentials irrespective of treatment assignment. $D_{2/3}R$ binding was assessed in the following brain regions: nucleus accumbens (NAC), caudateputamen (CP), thalamus (THAL), substantia nigra/ventral tegmental area (SN/VTA), frontal cortex (FC), motor cortex (MC), parietal cortec (PC), anterodorsal hippocampus (aHIPP) and posterior hippocampus (pHIPP).

	NAC	CP	THAL	SN/VTA	FC	MC	PC	aHIPP	pHIPP
NAC	0.000	0.566	0.000	0.114	0.000	0.000	0.000	0.000	0.146
CP		0.000	0.366	0.000	0.000	0.000	-0.098	0.000	0.000
THAL			0.000	0.062	0.000	0.000	0.000	0.346	0.046
SN/VTA				0.000	0.000	0.000	0.000	0.000	0.330
FC					0.000	0.414	0.081	0.000	0.000
MC						0.000	0.211	0.242	0.000
PC							0.000	0.000	0.000
aHIPP								0.000	0.076
pHIPP									0.000

Table 3: Path coefficient matrix after challenge with muscimol (MUS), bicuculline (BIC), D-cycloserine (DCS) and amantadine (AMA) obtained with mixed graphical modelling of $D_{2/3}R$ binding potentials (expressed as percentage of baseline). $D_{2/3}R$ binding was assessed in the following brain regions: nucleus accumbens (NAC), caudateputamen (CP), thalamus (THAL), substantia nigra/ventral tegmental area (SN/VTA), frontal cortex (FC), motor cortex (MC), parietal cortec (PC), anterodorsal hippocampus (aHIPP) and posterior hippocampus (pHIPP).

	NAC	CP	THAL	SN/VTA	FC	MC	PC	aHIPP	pHIPP
NAC									
MUS	0.000	0.323	0.000	0.000	0.000	0.000	0.000	0.000	0.000
BIC	0.000	0.744	0.000	0.000	0.000	0.000	0.000	0.000	0.000
DCS	0.000	0.396	0.000	0.000	0.000	0.000	0.000	0.000	0.000
AMA	0.000	0.472	0.000	0.122	0.000	0.000	0.000	0.000	0.000
CP									
MUS		0.000	0.459	0.000	0.000	0.000	0.000	0.000	0.000
BIC		0.000	0.000	0.000	0.000	0.000	0.000	0.000	0.000
DCS		0.000	0.000	0.000	0.000	0.000	0.000	0.000	0.000
AMA		0.000	0.175	0.163	0.000	0.000	0.000	0.000	0.000
THAL									
MUS			0.000	0.000	0.000	0.000	0.000	0.106	0.000
BIC			0.000	0.386	0.000	0.000	0.000	0.000	0.000
DCS			0.000	0.000	0.000	0.000	0.000	0.198	0.000
AMA			0.000	0.000	0.000	0.000	0.000	0.445	0.177
SN/VTA									
MUS				0.000	0.000	0.000	0.000	0.000	0.314
BIC				0.000	0.000	0.000	0.000	0.000	0.000
DCS				0.000	0.000	0.000	0.000	0.000	0.000
AMA				0.000	0.000	0.000	0.000	0.000	0.311
FC									
MUS					0.000	0.000	0.000	0.000	0.000
BIC					0.000	0.000	0.000	0.321	0.000
DCS					0.000	0.595	0.000	0.000	0.000
AMA					0.000	0.628	0.000	0.000	0.000
MC									
MUS						0.000	0.971	0.000	0.000
BIC						0.000	0.235	0.000	0.000
DCS						0.000	0.000	0.000	0.000
AMA						0.000	0.000	0.115	0.000
PC									
MUS							0.000	0.000	0.000
BIC							0.000	0.000	0.000
DCS							0.000	0.000	0.000
AMA							0.000	0.000	0.000
aHIPP									
MUS								0.000	0.000
BIC								0.000	0.000
DCS								0.000	0.000
AMA								0.000	0.000
pHIPP									
MUS									0.000
BIC									0.000
DCS									0.000
AMA									0.000

antagonistic (MUS/AMA) or $GABA_AR$ antagonistc and NMDAR agonistic (BIC/DCS) challenges pooled, six out of 36 possible connections for both MUS/AMA and BIC/DCS (sparsity: 0.833, each; Figure 6A and B, respectively, Table 4). After MUS and AMA combined, the strongest associations existed between FC and MC (c = 0.483), CP and THAL (c = 0.394) and MC and aHIPP (c = 0.222). After BIC and DCS combined, CP and NAC (c = 0.508), MC and PC (c = 0.475) and MC and FC (c = 0.284) were most strongly associated.

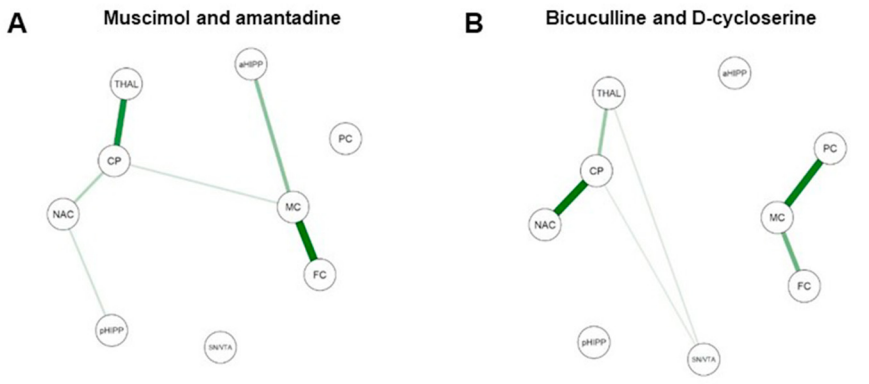

Figure 6: Connections between nucleus accumbes (NAC), caudeputamen (CP), thalamus (THAL), substantia nigra/ventral tegmental area (SN/VTA), FC, MC, parietal cortex (PC), anterodorsal hippocampus (aHIPP) and posterior hippocampus (pHIPP).
(A) Connections obtained after pooling of either $GABA_AR$ agonistic (muscimol) and NMDAR antagonistic challenge (amantadine) or (B) $GABA_AR$ antagonistic (bicuculline) and NMDAR agonistic challenge (D-cycloserine). Positive associations are represented by green lines. No negative associations were obtained. The size of the lines indicates the strength of the individual connections. Models were estimated with JASP (version 0.10.2.0, JASP Team, 2019, ©2013–2019 University of Amsterdam).

Table 4: Path coefficient matrix after pooling of $GABA_AR$ agonistic and NMDAR antagonistic (muscimol [MUS], amantadine [AMA]) as well as $GABA_AR$ antagonistc and NMDAR agonistic challenges (bicuculline [BIC], D-cycloserine [DCS]) obtained with mixed graphical modelling of $D_{2/3}R$ binding potentials (expressed as percentage of baseline). $D_{2/3}R$ binding was assessed in the following brain regions: nucleus accumbens (NAC), caudateputamen (CP), thalamus (THAL), substantia nigra/ventral tegmental area (SN/VTA), frontal cortex (FC), motor cortex (MC), parietal cortec (PC), anterodorsal hippocampus (aHIPP) and posterior hippocampus (pHIPP).

	NAC	CP	THAL	SN/VTA	FC	MC	PC	aHIPP	pHIPP
NAC									
MUS/AMA	0.000	0.156	0.000	0.000	0.000	0.000	0.000	0.000	0.017
BIC/DCS	0.000	0.508	0.000	0.000	0.000	0.000	0.000	0.000	0.000
CP									
MUS/AMA		0.000	0.394	0.000	0.000	0.100	0.000	0.000	0.000
BIC/DCS		0.000	0.208	0.077	0.000	0.000	0.000	0.000	0.000
THAL									
MUS/AMA			0.000	0.000	0.000	0.000	0.000	0.000	0.000
BIC/DCS			0.000	0.087	0.000	0.000	0.000	0.000	0.000
SN/VTA									
MUS/AMA				0.000	0.000	0.000	0.000	0.000	0.000
BIC/DCS				0.000	0.000	0.000	0.000	0.000	0.000
FC									
MUS/AMA					0.000	0.483	0.000	0.000	0.000
BIC/DCS					0.000	0.284	0.000	0.000	0.000
MC									
MUS/AMA						0.000	0.000	0.222	0.000
BIC/DCS						0.000	0.475	0.000	0.000
PC									
MUS/AMA							0.000	0.000	0.000
BIC/DCS							0.000	0.000	0.000
aHIPP									
MUS/AMA								0.000	0.000
BIC/DCS								0.000	0.000
pHIPP									
MUS/AMA									0.000
BIC/DCS									0.000

Discussion

Summary of findings

After treatment with the $GABA_AR$ agonistic MUS, $D_{2/3}R$ BP percentages of baseline were the lowest, followed by the NMDAR antagonistic AMA (with significant differences only in SN/VTA and PC). In turn, $D_{2/3}R$ BP percentages of baseline after treatment with the NMDAR agonistic DCS were the highest, followed by the $GABA_AR$ antagonistic BIC (with a significant difference only in PC). This implies that $GABA_AR$ agonist and NMDAR antagonist on one side and $GABA_AR$ antagonist and NMDAR agonist on the other induced similar effects on $D_{2/3}R$ binding and DA levels.

If we regard the significant differences relative to baseline after the individual pharmacological challenges, a pattern of region-specifity becomes apparent: while MUS reduced $D_{2/3}R$ binding (and increased DA levels) throughout the nigrostriatal and mesolimbic system (NAC, CP, SN/VTA, THAL and pHIPP), AMA-induced reductions of $D_{2/3}R$ binding (and elevations of DA) were confined to NAC, CP and THAL. Contrarily, while DCS augmented $D_{2/3}R$ binding (and decreased DA levels) throughout the nigrostriatal and mesolimbocortical (NAC, SN/VTA, THAL, FC, MC. PC, aHIPP and pHIPP), BIC-induced elevations of $D_{2/3}R$ binding (and decreases of DA) were limited to CP and THAL.

Both principal component and network analysis indicate intense functional relations between regions: the former identified $D_{2/3}R$ BPs (expressed as percentage of baseline) in CP (PrC1), SN/VTA (PrC2, PrC6), FC (PrC3), THAL (PrC4), PC (PrC5), MC (PrC7, PrC8) and NAC (PrC9) as the most prominent eigenvector components, which represented the very "nodes", between which the latter identified the majority of non-zero edges with path coefficients up to 0.971.

This poses the questions, how the DA-reducing effects of MUS and AMA and the DA-raising effects of BIC and DCS, their region-specifity and the apparent interactions between regions can be accounted for by the agonstic and antagonistic properties of these compounds.

$D_{2/3}R$ binding in baseline

In baseline, we assessed "normal" $D_{2/3}R$ binding in the individual brain regions without infliction of GABAergic or GLUergic challenges on DA function. As outlined above, the CP receives DAergic input from the SNc (Gerfen et al. 1987), GLUergic input form THAL and neocortex (Jayrayaman 1985; Smeal et al. 2007) and GABAergic input from the neocortex (Lee et al. 2014), while it sends GABAergic efferents to GPi, GPe and SN (Hattori et al. 1975; Graybiel and Ragsdale 1979; Bolam et al. 1981). Via the direct and indirect pathway, GPi and GPe provide GABAergic input to THAL and STN (Albin et al. 1989). The THAL sends further GLUergic efferents to the neocortex (Kharazia and Weinberg 1994), whereas the STN routes GLUergic fibers to the VP, as well as back to GP and SN (Carpenter et al. 1981; Albin et al. 1989; Turner et al. 2001). The NAC receives DAergic input from VTA (Lisman and Grace 2005), GLUergic input from THAL, PFC and HIPP (Walaas and Fonnum 1988a0; Jayrayaman 1985; Berendse et al. 1992) and GABAergic input from VTA and PFC (Brown et al. 2012; Lee et al. 2014), while it sends GABAergic efferents to VP and SN as well as back to the VTA (Nauta and Vole 1978; Walaas and Fonnum 1980b). The VP, in turn, provides GABAergic input to the THAL (Kuo and Carpenter 1973) and back to the VTA (Lisman and Grace 2005).

The network analysis of regional BPs in baseline yielded positive associations between $D_{2/3}R$ binding (and DA levels) in CP and NAC, CP and THAL, THAL and aHIPP, NAC and SN/VTA, NAC and pHIPP, SN/VTA and pHIPP, aHIPP and MC, MC and PC, MC and FC and FC and PC. Since all of these regions are either directly or indirectly linked (see above), the model obtained by network analysis of $D_{2/3}R$ binding in baseline provides a suitable standard for the subsequent analyses of DA function after the indivdual GABAergic and GLUergic challenges.

$D_{2/3}R$ binding after the individual GABAergic and GLUergic challenges

MUS After treatment with the $GABA_AR$ agonistic MUS, network analysis of the regional BPs (expressed as percentage of baseline) yielded positive associations between $D_{2/3}R$ binding in CP and THAL, CP and NAC, SN/VTA and pHIPP and MC and PC. Thus, percentual reductions of $D_{2/3}R$ binding (and increases of DA) relative to baseline in CP, SN/VTA and MC were accompanied by percentual reductions of $D_{2/3}R$ binding (and increases of DA) in THAL, NAC, pHIPP and PC, respectively, and vice versa. This direct relationship is plausible, since the effects of MUS on $D_{2/3}R$ binding (and DA levels) are unidirectional and lie in the same order of magnitude across regions.

In order to account for these findings, we propose the following mechanism of action: the increased $GABA_AR$ agonistic action in the CP may be conceived to inhibit the SN via striatonigral GABAergic projections. Increased inhibition of GPi and GPe via GABAergic striatopallidal fibers

lead to a disinhibition of SN and THAL. The consequence is an increase of nigral and thalamic DA, as reflected by the reduction of $D_{2/3}R$ binding under the above experimental conditions.

From the THAL, GLUergic efferents run to the neocortex (Jarayaman 1985), which, in turn, sends GLUergic projections back to the CP (Kharazia and Weinberg 1994). Disinhibition of the THAL elevates GLUergic excitation of the neocortex, enhancing the excitatory input of corticostriatal fibers. Excitatory GLUergic afferents likely compensate the $GABA_AR$ agonistic action in the CP, leading to the elevation of neostriatal DA concentrations reflected by the observed reduction of $D_{2/3}R$ binding.

The NAC receives inhibitory GABAergic afferents from PFC (Lee et al. 2014) and VTA (Brown et al. 2012) and sends GABAergic efferents back to the VTA (Watabe-Uchida et al. 2012) as well as to the VP (Nauta and Cole 1978), which, in turn provides GABAergic input to THAL (Kuo and Carpenter 1973) and VTA (Lisman and Grace 2005). In line with the action of MUS on the CP (incurring elevated inhibition of the SN), the action of MUS on the NAC may be conceived to enhance the inhibition of the VTA. However, in analogy to the CP, the disinhibition of the THAL increases GLUergic input to the neocortex and, via GLUergic efferents, back to the NAC, leading to the elevation of ventrostriatal DA concentrations as reflected by the observed reduction of $D_{2/3}R$ binding. Moreover, the disinhibition of the VTA may incur a net increase of endogenous DA as reflected by the observed reduction of $D_{2/3}R$ binding.

The HIPP receives DAergic neurons originating in the VTA (Gasparri et al. 1991). Since the increased excitation of the NAC can be assumed to enhance the DAergic input back to the VTA, the likely consequence is also an increase of DAergic input to the HIPP, leading to the observed reduction of $D_{2/3}R$ binding.

BIC After treatment with the $GABA_AR$ antagonistic BIC, network analysis of the regional BPs (expressed as percentage of baseline) yielded positive associations between $D_{2/3}R$ binding in CP and NAC, SN/VTA and THAL, FC and aHIPP and MC and PC. Thus, percentual elevations of $D_{2/3}R$ binding (and decreases of DA) relative to baseline in CP, SN/VTA, FC and MC are accompanied by percentual elevations of $D_{2/3}R$ binding (and decreases of DA) in NAC, THAL, aHIPP and PC, respectively, and vice versa.

In vivo imaging studies did not show alterations of $D_{2/3}R$ binding (and DA) in SN/VTA, NAC, neocortex and HIPP. Hence, the DAergic input to the CP via ascending nigrostriatal fibers can be assumed to be normal. Based on the observed augmentation of $D_{2/3}R$ binding in the CP, however, it may be inferred that GPi and GPe receive increased $GABA_AR$ antagonistic input from the CP, leading to the inhibition of the THAL. This, for one, may account for the decrease of thalamic DA levels reflected by the observed increase of $D_{2/3}R$ binding in this region.

The elevation of inhibitory GABAergic input to the THAL, secondly, can be surmised to diminish not only the direct GLUergic input to the CP, but also the excitatory input to the neocortex, which sends GLUergic efferents back to the CP. It may be hypothesized that the increase of DA efflux effected by the elevation of the $GABA_AR$ antagonistic action in the CP is outweighed by the decline of excitatory input from THAL and neocortex, leading to a net decrease of available DA as reflected by the observed increase of $D_{2/3}R$ binding.

It is interesting that network analysis did not yield a direct connection between CP and THAL after BIC. Rather, positive associatons between CP and NAC as well as THAL and SN/VTA were obtained, with $D_{2/3}R$ binding (and DA levels) in NAC and SN/VTA, however, not affected by BIC challenge. This, likewise, holds for MC and PC, as well as FC and aHIPP, which were positively associated, but also failed to show alterations of $D_{2/3}R$ binding after treatment with BIC. It may be concluded that the decreases of nigrostriatal and thalamic DA were functionally related to decreases of DA levels in SN/VTA, NAC, neocortex and aHIPP, which were, however, too low to induce measurable changes of $D_{2/3}R$ binding under the present experimental conditions.

DCS After challenge with the NMDAR agonistic DCS, network analysis of the regional BPs (expressed as percentage of baseline) yielded positive associations between $D_{2/3}R$ binding in CP and NAC, THAL and aHIPP and FC and MC. Consequently, percentual increases of $D_{2/3}R$ binding (and reductions of DA) relative to baseline in CP, THAL and FC are accompanied by percentual increases of $D_{2/3}R$ binding (and reductions of DA) in NAC, aHIPP and MC, respectively, and vice versa.

DCS elevates GABA release in the mouse whole brain (Polc et al. 1986, Scotto et al. 1963). Moreover, decreased GLU levels were observed in the rat amygdala (Lehner et al. 2010) as well as in the mouse whole brain (Polc et al. 1986), whereas no effect was detected in the rat FC (Fujihira et al. 2007). Thus, after DCS, increased GABAergic input from striato- as well as pallidonigral fibers may be inferred, which, together with decreased GLUergic input from the STN, results in a net inhibition of the SN. Additionally, the VTA receives increased GABAergic input from the NAC, which, in turn, is subject to decreased GLUergic input from both neocortex and HIPP. In sum, this may ensue in a decrease of DA concentrations in SN/VTA, as reflected by the observed increase of $D_{2/3}R$ binding in this target region.

The decline of DA levels in SN and VTA diminishes the DAergic input to both CP and NAC. In the NAC, this - together with the reduced GLUergic input from both neocortex and limbic system – may be expected to incur a net reduction of available DA, as reflected by the augmentation of $D_{2/3}R$ binding in the present study.

The CP not only receives DAergic afferents from the SNc, but also GLUergic fibers from PFC, FC, MC, somatosensory cortex and THAL (for review see Afifi et al. 1994a,b). The DCS-induced decline of GLU efflux results in a decrease of GLUergic input (except for the FC [Fujihira et al. 2007]). Together with the increased availability of inhibitory GABA in the neostriatal microcircuits (Groves 1983), this can be hypothesized to reduce DA levels in the CP, in analogy to the NAC. However, thalamic disinhibition exerted by increased GABA levels in the direct and indirect pathway, apparently, fascilitates GLUergic stimulation of the CP, leading to a compensatory enhancement of DA release, and, ultimately, to unaltered neostriatal $D_{2/3}R$ binding in the CP under the present experimental conditions.

Since GLUergic input from the THAL to the neocortex may be decreased, a likely consequence is the decline of neocortical DA levels, as reflected by the observed decreases of $D_{2/3}R$ binding in FC, MC and PC. In turn, in the THAL, decreased GLUergic input from the neocortex may outweigh the disinhibition exerted via the pallidothalamic pathway, leading to a reduction of DA levels, as reflected by the increase of $D_{2/3}R$ binding in this region.

The decline of GLU release in neocortical and limbic regions as well as the decrease of DAergic input to the HIPP via ventral tegmental afferents may be inferred to diminish DAergic input to the limbic system, leading to a decrease of hippocampal DA levels, as reflected by the observed increase of $D_{2/3}R$ binding in aHIPP and pHIPP.

Strikingly, in spite of the increase of $D_{2/3}R$ binding (and decrease of DA) throughout the nigrostriatal and mesolimbic system and the possibility to account for these findings by the known interactions between DA, GLU, GABA in the individual brain regions, network analysis merely yielded direct connections between CP (whose $D_{2/3}Rs$ were not measurably affecteld by DCS) and NAC, THAL and aHIPP as well as FC and MC. Evidently, the NMDAR agonistic DCS elicited regional alterations of DA levels, which were not strictly interdependent and presumably involved neurotransmitter actions beyond DA, GLU and GABA, which werely solely considered in our model.

AMA After challenge with the NMDAR antagonistic AMA, network analysis of the regional BPs (expressed as percentage of baseline) yielded positive associations between $D_{2/3}R$ binding in CP and NAC, CP and THAL, CP and SN/VTA, NAC and SN/VTA, THAL and aHIPP, THAL and pHIPP, SN/VTA and pHIPP, FC and MC as well as MC and aHIPP. Thus, percentual reductions of $D_{2/3}R$ binding (and increases of DA) relative to baseline in CP are accompanied by percentual reductions of $D_{2/3}R$ binding (and increases of DA) in NAC, THAL and SN/VTA and vice versa. Likewise, percentual reductions of $D_{2/3}R$ binding (and increases of DA) relative to baseline in NAC, THAL and SN/VTA are directly related to percentual reductions of $D_{2/3}R$ binding (and increases of DA) in SN/VTA and both aHIPP and pHIPP, respectively. Furthermore, percentual reductions of $D_{2/3}R$ binding (and increases of DA) relative to baseline in FC and MC are accompanied by percentual reductions of $D_{2/3}R$ binding (and increases of DA) relative to baseline in MC and aHIPP, respectively.

AMA enhances both GABA (Bak et al. 1972) and GLU efflux (Takahashi et al. 1996) in the CP. Hence, for one, the increased availability of inhibitory GABA in the neostriatal microcircuits (Groves 1983) may be conceived to incur a reduction of DA efflux in the CP. Moreover, it can be surmised that AMA fascilitates the release of GABA in the NAC, reducing available DA also in the latter region. On the other hand, however, both CP and NAC receive GLUergic afferents, and it may be hypothesized that the augmentation of GLUergic input outweighs the action of GABA, resulting in a net elevation of DA levels in CP and NAC, as reflected by the decline of $D_{2/3}R$ binding observed in these regions. Thereby, however, DA levels in both CP and NAC, after AMA, fall short by one order of magnitude compared to MUS. This may be accounted for, firstly, by different extents of GABAergic action exerted by MUS and AMA, and, secondly, by the lack of DA increase in SN/VTA after AMA, likely incurring less DAergic input into the dorso- and ventrostriatal target regions of nigral and ventral tegmental projections.

As outlined above for MUS, the AMA-induced increase of GABA levels in the CP enhances the inhibition of GPi and GPe via striatopallidal GABAergic projections. Increased inhibition of the GP ensues in a net disinhibition of the THAL, resulting in the increase of thalamic DA reflected by the reduction of $D_{2/3}R$ binding under the present experimental conditions. With DA levels in the CP lower after AMA compared to MUS, it may be argued that, on account of this fact, also thalamic DA levels are lower.

It is remarkable that network analysis not only yielded connections between CP, NAC and THAL but also between

these regions and SN/VTA, aHIPP and pHIPP. Also here, it may be implied that the NMDAR antagonistic AMA elicited regional alterations of DA levels, which, however, were not sufficient to induce measurable reductions of $D_{2/3}R$ binding.

$D_{2/3}R$ binding after pooling of of treatments

MUS and AMA After combination of the $GABA_AR$ agonistic MUS and the NMDAR antagonistic AMA, network analysis yielded positive associations between $D_{2/3}R$ binding in CP and THAL, CP and NAC, CP and MC, NAC and pHIPP, MC and FC as well as MC and pHIPP. Thus, percentual reductions of $D_{2/3}R$ binding (and increases of DA) relative to baseline in CP were accompanied by percentual reductions of $D_{2/3}R$ binding (and increases of DA) in THAL, NAC and MC. Likewise, percentual reductions of $D_{2/3}R$ binding (and increases of DA) relative to baseline in NAC and MC were related to percentual reductions of $D_{2/3}R$ binding in pHIPP and in CP, aHIPP and FC, respectively.

Thus, appararently, many regulatory effects on DA levels are common to MUS and AMA. Interestingly, however, after pooling of MUS and AMA, the connections between SN/VTA and pHIPP as well as SN/VTA and pHIPP and both dorsal and ventral striatum were obliterated, which formerly had been obtained by separate analysis of binding data after MUS and AMA challenge, respectively. This is primarily due to the fact that, in contrast to MUS, AMA did not increase DA levels in SN/VTA. After MUS, increased inhibition of GPi and GPe lead to a disinhibition of the SN, resulting in the increase of nigral DA. Likewise, the disinhibition of the THAL increases GLUergic input to the neocortex and, via GLUergic efferents, back to the NAC, leading to an enhancement of DA efflux in the VTA. After AMA, however, synaptic DA is lower in CP, NAC and THAL compared to MUS. As mentioned above, this, for one, may be due to different extents of GABAergic action after MUS and AMA. Furthermore, the NMDAR antagonst, in contrast to MUS, is known to facilitate neostriatal GLU release (Takahashi et al. 1996). Apparently, in sum, the ensuing effects balance each other, leaving $D_{2/3}R$ binding in SN/VTA unaltered relative to baseline.

Furthermore, in contrast, to MUS, AMA did not increase DA levels in pHIPP. As outlined above, after MUS, the increased excitiation of the VTA likely enhances the DAergic input to the HIPP. Since challenge with AMA, however, incurs no alterations of synaptic DA levels in SN/VTA, also no alterations of hippocampal DA levels are likely to occur.

BIC and DCS After combination of $GABA_AR$ antagonistic and NMDAR agonistic treatment, network analysis yielded positive associations between $D_{2/3}R$ binding in CP and NAC, CP and THAL, CP and SN/VTA, THAL and SN/VTA, MC and FC as well as MC and FC. Thus, percentual reductions of $D_{2/3}R$ binding (and increases of DA) relative to baseline in CP were accompanied by percentual reductions of $D_{2/3}R$ binding (and increases of DA) in NAC, THAL and SN/VTA. Likewise, percentual reductions of $D_{2/3}R$ binding (and increases of DA) relative to baseline in SN/VTA and MC were related to percentual reductions of $D_{2/3}R$ binding in CP and THAL as well as FC and PC, respectively. When comparing these connections with the ones obtained after separate analyses of binding data after BIC and DCS challenge, respectively, it becomes obvious that a connection between SN/VTA and CP was added, while connections between FC and aHIPP THAL and pHIPP were obliterated. Again, this may be accounted for by the differing effects of BIC and DCS on regional $D_{2/3}Rs$.

In contrast to BIC, DCS increased $D_{2/3}R$ binding (and decreased DA) thoughout the nigrostriatal and mesolimbic system except for the CP. DCS elevates GABA release in the mouse whole brain (Polc et al. 1986, Scotto et al. 1963), hence, for DCS, it may be assumed that the availability of inhibitory GABA is increased in the neostriatal microcircuits (Groves 1983), which ought to diminish DA levels in the CP, but is outweighed by thalamic disinhibition exerted by increased GABA levels in the direct and indirect pathway, leading to a compensatory enhancement of DA release, and, ultimately, to unaltered neostriatal $D_{2/3}R$ binding in the CP. Contrarily, for BIC, it may be hypothesized that the increase of DA efflux effected by the elevation of the $GABA_AR$ antagonistic action in the CP is outweighed by the decline of excitatory input from THAL and neocortex, leading to a net decrease of available DA and the observed elevation of $D_{2/3}R$ binding.

Moreover, after BIC, DA levels in SN/VTA remained normal, also resulting in normal neocortical $D_{2/3}R$ binding. In contrast, after DCS, a decline of GLU efflux (Polc et al. 1986) may have incurred a net reduction of neocortical DA levels, as reflected by the observed decreases of $D_{2/3}R$ in FC, MC and PC.

After BIC, normal DA levels in SN/VTA also incurred a normal DAergic input to the limbic system. In contrast, after DCS, DA levels in SN/VTA were diminished, which, together with the DCS-induced reduction of GLU release in neocortical and limbic regions may have incurred the decrease of hippocampal DA levels, as reflected by the observed increase of $D_{2/3}R$ binding in aHIPP and pHIPP.

Conclusions

The reductions of $D_{2/3}R$ binding after MUS and AMA (in the present doses) indicate increased DA levels in the nigrostriatal and mesolimbic system, whereas, contrarily, the increases of $D_{2/3}R$ binding after DCS and BIC (in the present doses) reflect reductions of available DA in the nigrostriatal and throughout the mesolimbocortical system, respectively.

Network analysis yielded an association between $D_{2/3}R$ binding (and DA levels) in CP and THAL, which is in line with the known neuronal connections between these regions. The obtained association was strongest in baseline, moderate after challenge with the $GABA_AR$ agonistic MUS and weakest after challenge with the NMDAR antagonistic AMA, which may be conceived to reflect the decline of DA release elicited by the increase of inhibitory $GABA_AR$ as well as the decrease of excitatory NMDAR action. Interestingly, the association between CP and THAL is unhinged by treatment with both the $GABA_AR$ antagonistic BIC and the NMDAR agonistic DCS, which both induce a decline of thalamic DA as evidenced by the elevation of $D_{2/3}R$ binding in this region.

Moreover, network analysis demonstrated a functional association between $D_{2/3}R$ binding (and DA levels) in CP and NAC, which was strongest in baseline and after challenge with BIC, moderate after challenge with AMA and DCS and weakest after challenge with MUS. Apparently, DA efflux in CP and NAC still correlate after $GABA_AR$ antagonistic treatment as much as they do in the untreated animal, while this connection, interestingly, deteriorates after pharmacologically induced alterations of GLUergic neurotransmission as well as after $GABA_AR$ agonistic treatment.

SN/VTA, the site of origin of DAergic fibers, and its neostriatal target region, interestingly, exhibit a strong association after challenge with the NMDAR antagonistic AMA. The apparent correlation between DA efflux in SN/VTA and CP, however, neither exists in baseline, where GLUergic neurotransmission is not one-sidedly challenged, nor after treatment with the NMDAR agonistic DCS or the GABAergic compounds MUS and BIC. In contrast, SN/VTA and NAC exhibit a low association not only after challenge with AMA, but also in baseline, which, however, is likewise disrupted after treatment with the NMDAR agonistic DCS and the GABAergic compounds MUS and BIC.

Another striking feature is the strong association between SN/VTA and THAL after challenge with the $GABA_AR$ antagonistic BIC, which – in accordance with the connection between SN/VTA and CP - is not present in baseline. In contrast to the connection between SN/VTA and CP, however, it is disrupted by treatment with the $GABA_AR$ agonistic MUS and the NMDAergic compounds AMA and DCS.

The association between THAL and aHIPP was strongest after challenge with AMA, moderate after challenge with DCS, but unhinged in baseline and after challenge with the GABAergic compounds. Network analysis, furthermore, yielded a strong association between $D_{2/3}R$ binding (and DA levels) in MC and FC, which was strongest after treatment with AMA and DCS, slighly weaker in baseline and completely disrupted after challenge with the GABAergic compounds. In contrast, after MUS, a strong association was observed between MC and PC, which was weaker in baseline and after treatment with BIC, but completely disrupted after challenge with the GLUergic compounds.

Altogether, this underlines that the effects of $GABA_AR$ and NMDAR agonists and antagonists on DA function are region-specific. Although $GABA_AR$ agonist and NMDAR antagonist on one side and $GABA_AR$ antagonist and NMDAR agonist on the other side uniformly affect $D_{2/3}R$ binding (and DA levels), the extent of involved brain regions varies with a significant impact beyond ventral and/or dorsal striatum plus THAL only after (either $GABA_AR$ or NMDAR) agonistic treatment.

In the present series of experiments, the maximum VOI diameters were either in the range of or beyond the spatial resolution of the "TierSPECT" (Nikolaus et al. 2018a). It must be taken into consideration, however, that in those portions of VOIs, whose diameters were smaller than the full width at half maximum, the quantification of $D_{2/3}R$ binding may have been confounded by partial volume effects leading to underestimations of radioligand accumulation. On the other hand, spill-over from regions with high radioligand accumulation to adjacent VOIs may have caused overestimations of regional radioligand binding. However, since this held for SPECT measurements both in baseline and post-challenge, the exactitude of (semi) quantitative values in either condition, but not the comparability of data between baseline and challenge may have been biassed. Another pitfall of the present studies may have been the employment of the NMDAR antagonist ketamine as anaesthetic. Since ketamine may increase DA release in rats (Onoe et al. 1994), it can not be dismissed that increased amounts of DA due to ketamine action actually diminished regional $D_{2/3}$ receptor binding after challenge with MUS, BIC, DCS and AMA. Effects on neostriatal and/or ventrostriatal DA, however, are exerted by practically all known anaesthetics (for review see Müller

et al. 2011), and since the same anaesthetic was used in baseline and post-challenge, data basically remain comparable not also between baseline and challenge but also between the individual pharmacological treatments.

The most important limitation, however, is that in the present imaging studies only the action of GABAergic and GLUergic challenges on DA have been assessed. Since also effects of serotonin (Saito et al. 1996), acetylcholine (Marshall et al. 1997) and/or substance P (Hasenöhrl et al. 2000) on cerebral DA are widely known - not to mention their interactions with GABA and GLU (see, e. g., Aghajanian and Marek 1999; Cathala et al. 2019; Hu et al. 2004; Howe et al. 2016; Xia et al. 2010; Yousefi et al. 2012) - the performance of further receptor (beyond $D_{2/3}$Rs) and transporter imaging studies is mandatory, in which neurotransmitter systems beyond GLU and GABA are challenged.

Author contribution: All the authors have accepted responsibility for the entire content of this submitted manuscript and approved submission.
Research funding: None declared.
Employment or leadership: None declared.
Honorarium: None declared.
Conflict of interest statement: The authors declare no conflicts of interest regarding this article.

References

Afifi, A.K. (1994a). Basal ganglia: functional anatomy and physiology. Part 1. J. Child Neurol. 9: 249–260.

Afifi, A.K. (1994b). Basal ganglia: functional anatomy and physiology. Part 2. J. Child Neurol. 9: 352–361.

Aghajanian, G.K. and Marek, G.J. (1999). Serotonin, via 5-HT2A receptors, increases EPSCs in layer V pyramidal cells of prefrontal cortex by an asynchronous mode of glutamate release. Brain Res 825: 161–171.

Albin, R.L., Young, A.B. and Penney, J.B. (1989). The functional anatomy of basal ganglia disorders. Trends Neurosci 12: 366–375.

Aono, Y., Saigusa, T., Mizoguchi, N., Iwakami, T., Takada, K., Gionhaku, N., Oi, Y., Ueda, K., Koshikawa, N., and Cools, A.R. (2008). Role of GABAA receptors in the endomorphin-1-, but not endomorphin-2-, induced dopamine efflux in the nucleus accumbens of freely moving rats. Eur. J. Pharmacol. 580: 87–94.

Bak, I.J., Hassler, R., Kim, J.S. and Kataoka, K. (1972). Amantadine actions on acetylcholine and GABA in striatum and substantia nigra of rat in relation to behavioral changes. J Neural Transm 33: 45–61.

Bennett, S. and Gronier, B. (2005). Modulation of striatal dopamine release in vitro by agonists of the glycineB site of NMDA receptors; interaction with antipsychotics. Eur. J. Pharmacol. 527: 52–59.

Berendse, H.W., Galis-de Graaf, Y. and Groenewegen, H.J. (1992). Topographical organization and relationship with ventral striatal compartments of prefrontal corticostriatal projections in the rat. J. Comp. Neurol. 316: 314–347.

Bolam, J.P., Powell, J.F., Totterdell, S. and Smith, A.D. (1981). The proportion of neurons in the rat neostriatum that project to the substantia nigra demonstrated using horseradish peroxidase conjugated with wheatgerm agglutinin. Brain Res 220: 339–343.

Bouthenet, M.L., Martres, M.P., Sales, N. and Schwartz, J.C. (1987). A detailed mapping of dopamine D-2 receptors in rat central nervous system by autoradiography with [125I]iodosulpride. Neuroscience 20: 117–155.

Bromberg, M.B., Penney, J.B., Jr., Stephenson, B.S. and Young, A.B. (1981). Evidence for glutamate as the neurotransmitter of corticothalamic and corticorubral pathways. Brain Res 215: 369–374.

Brown, M.T., Tan, K.R., O'Connor, E.C., Nikonenko, I., Muller, D. and Lüscher, C. (2012). Ventral tegmental area GABA projections pause accumbal cholinergic interneurons to enhance associative learning. Nature 492: 452–456.

Carpenter, M.B., Baton, R.R., 3rd, Carleton, S.C. and Keller, J.T. (1981). Interconnections and organization of pallidal and subthalamic nucleus neurons in the monkey. J. Comp. Neurol. 197: 579–603.

Carr, D.B. and Sesack, S.R. (2000). GABA-containing neurons in the rat ventral tegmental area project to the prefrontal cortex. Synapse 38: 114–123.

Cathala, A., Devroye, C., Drutel, G., Revest, J.M., Artigas, F. and Spampinato, U. (2019). Serotonin$_{2B}$ receptors in the rat dorsal raphe nucleus exert a GABA-mediated tonic inhibitory control on serotonin neurons. Exp. Neurol. 311: 57–66.

Cobb, W.S. and Abercrombie, E.D. (2002). Distinct roles for nigral GABA and glutamate receptors in the regulation of dendritic dop amine release under normal conditions and in response to systemic haloperidol. J. Neurosci. 22: 1407–1413.

Cobb, W.S. and Abercrombie, E.D. (2003). Relative involvement of globus pallidus and subthalamic nucleus in the regulation of somatodendritic dopamine release in substantia nigra is dopamine-dependent. Neuroscience 119: 777–786.

Corbett, R., Fielding, S., Cornfeldt, M. and Dunn, R.W. (1991). GABAmimetic agents display anxiolytic-like effects in the social interaction and elevated plus maze procedures. Psychopharmacology (Berl) 104: 312–316.

Fujihira, T., Kanematsu, S., Umino, A., Yamamoto, N. and Nishikawa T. (2007). Selective increase in the extracellular D-serine contents by D-cycloserine in the rat medial frontal cortex. Neurochem. Int. 51: 233–236.

Gandolfi, O., Rimondini, R. and Dall'Olio, R. (1994). D-cycloserine decreases both D1 and D2 dopamine receptors number and their function in rat brain. Pharmacol. Biochem. Behav. 48: 351–356.

Gasbarri, A., Campana, E., Pacitti, C., Hajdu, F. and Tömböl, T. (1991). Organization of the projections from the ventral tegmental area of Tsai to the hippocampal formation in the rat. J. Hirnforsch. 32: 429–437.

Gerfen, C.R., Herkenham, M. and Thibault, J. (1987). The neostriatal mosaic: II. Patch- and matrix-directed mesostriatal dopaminergic and non-dopaminergic systems. J. Neurosci. 7: 3915–3934.

Girardi, E. and Rodríguez de Lores Arnaiz, G. (1987). Citrate synthase and lactate dehydrogenase activities in rat cerebral cortex

following the administration of the convulsants bicuculline and 3-mercaptopropionic acid. Acta Physiol. Pharmacol. Latinoam. 37: 235–243.
Graybiel, A.M. and Ragsdale, C.W., Jr. (1979). Fiber conncetions of the basal ganglia. Prog. Brain Res. 51,237–283.
Groves, P.M. (1983). A theory of the functional organization of the neostriatum and the neostriatal control of voluntary movement. Brain Res. 5, 109–132.
Hasenöhrl, R.U., Souza-Silva, M.A., Nikolaus, S., Tomaz, C., Brandao, M.L., Schwarting, R.K. and Huston, J.P. (2000). Substance P and its role in neural mechanisms governing learning, anxiety and functional recovery. Neuropeptides 34: 272–280.
Haslbeck, J.M.B. and Waldorp, L.J. (2015). mgm: Estimating time-varying mixed graphical models in high-dimensional data. arXIV: 1510.06871 [stat.AP].
Hattori, T., Fibiger, H.C. and McGeer, P.L. (1975). Demonstration of a pallido-nigral projection innervating dopaminergic neurons. J. Comp. Neurol 162: 487–504.
Hotelling, H. (1933). Analysis of a complex of statistical variables into principle components. J. Edu. Psychol 24: 417–41.
Howe, W.M., Young, D.A., Bekheet, G. and Kozak, R. (2016). Nicotinic receptor subtypes differentially modulate glutamate release in the dorsal medial striatum. Neurochem. Int 100: 30–34.
Hu, H.J., Chen, L.W., Yung, K.K. and Chan, Y.S. (2004). Differential expression of AMPA receptor subunits in substance P receptor-containing neurons of the caudate-putamen of rats. Neurosci. Res 49: 281–288.
Ichise, M., Meyer, J.H. and Yonekura, Y. (2001). An introduction to PET and SPECT neuroreceptor quantification models. J. Nucl. Med. 42: 755–763.
Ikemoto, S., Kohl, R.R. and McBride, W.J. (1997). GABA(A) receptor blockade in the anterior ventral tegmental area increases extracellular levels of dopamine in the nucleus accumbens of rats. J. Neurochem. 69: 137–143.
Ito, Y., Lim, D.K., Hoskins, B. and Ho, I.K. (1988). Bicuculline up-regulation of GABAA receptors in rat brain. J. Neurochem. 51: 145–152.
JASP Team (2019). JASP (Version 0.10.2) [Computer software].
Jayaraman, A. (1985). Organization of thalamic projections in the nucleus accumbens and the caudate nucleus in cats and its relation with hippocampal and other subcortical afferents. J. Comp. Neurol. 231: 396–420.
Karreman, M. and Moghaddam, B. (1996). The prefrontal cortex regulates the basal release of dopamine in the limbic striatum: an effect mediated by ventral tegmental area. J. Neurochem. 66: 589–598.
Kharazia, V.N. and Weinberg, R.J. (1994). Glutamate in thalamic fibers terminating in layer IV of primary sensory cortex. J. Neurosci. 14: 6021–6032.
Kornhuber, J., Bormann, J., Hübers, M., Rusche, K. and Riederer, P. (1991). Effects of the 1-amino-adamantanes at the MK-801-binding site of the NMDA-receptor-gated ion channel: a human postmortem brain study. Eur. J. Pharmacol. 206: 297–300.
Kornhuber, J., Schoppmeyer, K., Riederer, P. (1993). Affinity of 1-aminoadamantanes for the sigma binding site in post-mortem human frontal cortex. Neurosci. Lett. 163: 129–131.
Kuo, J.S. and Carpenter, M.B. (1973). Organization of pallidothalamic projections in the rhesus monkey. J. Comp. Neurol. 151: 201–236.
Laruelle, M. (2000). Imaging synaptic neurotransmission with in vivo binding competition techniques: a critical review. J. Cereb. Blood Flow Metab. 20: 423–451.
Lee, A.T., Vogt, D., Rubenstein, J.L. and Sohal, V.S. (2014). A class of GABAergic neurons in the prefrontal cortex sends long-range projections to the nucleus accumbens and elicits acute avoidance behavior. J. Neurosci. 34: 11519–11525.
Lehne, M., Wisłowska-Stanek, A., Taracha, E., Maciejak, P., Szyndler, J., Skórzewska, A., Turzyńska, D., Sobolewska, A., Hamed, A., Bidziński, A. and Płaźnik, A. (2010). The effects of midazolam and D-cycloserine on the release of glutamate and GABA in the basolateral amygdala of low and high anxiety rats during extinction trial of a conditioned fear test. Neurobiol Learn Mem. 94: 468–480.
Lindvall, O. and Björklund, A. (1974). The organization of the ascending catecholamine neuron systems in the rat brain as revealed by the glyoxylic acid fluorescence method. Acta Physiol. Scand. (Suppl.) 412: 1–48.
Lindvall, O. and Björklund, A. (1978). Anatomy of the dopaminergic neuron systems in the rat brain. Adv. Biochem. Psychopharmacol. 19, 1–23.
Lisman, J.E. and Grace, A.A. (2005). The hippocampal-VTA loop: controlling the entry of information into long-term memory. Neuron 46: 703–713.
Maj, J., Sowińska, H. and Baran, L. (1972). The effect of amantadine on motor activity and catalepsy in rats. Psychopharmacologia 24: 296–307.
Marshall, D.L., Redfern, P.H. and Wonnacott, S. (1997). Presynaptic nicotinic modulation of dopamine release in the three ascending pathways studied by in vivo microdialysis: comparison of naive and chronic nicotine-treated rats. J Neurochem. 68: 1511–1519.
Matsumoto, M., Kanno, M., Togashi, H., Ueno, K., Otani, H., Mano, Y. and Yoshioka, M. (2003). Involvement of GABAA receptors in the regulation of the prefrontal cortex on dopamine release in the rat dorsolateral striatum. Eur. J. Pharmacol. 482: 177–184.
Monahan, J.B., Handelmann, G.E., Hood, W.F. and Cordi, A.A. (1989). D-cycloserine, a positive modulator of the N-methyl-D-aspartate receptor, enhances performance of learning tasks in rats. Pharmacol. Biochem. Behav. 34: 649–653.
Monakow, K.H., Akert, K. and Künzle, H. (1978). Projections of the precentral motor cortex and other cortical areas of the frontal lobe to the subthalamic nucleus in the monkey. Exp. Brain Res. 33, 395–403.
Morelli, M., Mennini, T., Cagnotto, A., Toffano, G. and Di Chiara, G. (1990). Quantitative autoradiographical analysis of the age-related modulation of central dopamine D1 and D2 receptors. Neuroscience 36: 403–410.
Moresco, R.M., Volonte, M.A., Messa, C., Gobbo, C., Galli, L., Carpinelli, A., Rizzo, G., Panzacchi, A., Franceschi, M. and Fazio, F. (2002). New perspectives on neurochemical effects of amantadine in the brain of parkinsonian patients: a PET - [(11)C] raclopride study. J. Neural Transm. (Vienna) 109: 1265–1274.
Müller, C.P., Pum, M.E., Amato, D., Schüttler, J., Huston, J.P. and Silva, M.A. (2011). The in vivo neurochemistry of the brain during general anesthesia. J. Neurochem. 119: 419–446.
Nauta, H.J. and Cole, M. (1978). Efferent projections of the subthalamic nucleus: an autoradiographic study in monkey and cat. J. Comp. Neurol. 180: 1–16.
Negro, M., Chinchetru, M.A., Fernández, A. and Calvo, P. (1995). Effect of ethanol treatment on rate and equilibrium constants for [^{3}H] muscimol binding to rat brain membranes: alteration of two affinity states of the $GABA_A$ receptor. J. Neurochem. 64: 1379–1389.

Nikolaus, S., Antke, C. and Müller, H.W. (2009a). *In vivo* imaging of synaptic function in the central nervous system. I. Movement disorders and dementia. Behav. Brain Res. 204: 1–31.

Nikolaus, S., Antke, C. and Müller, H.W. (2009b). In vivo imaging of synaptic function in the central nervous system. II. Mental and affective disorders. Behav. Brain Res. 204: 32–66.

Nikolaus, S., Beu, M., Antke, C. and Müller, H.W. (2010). Cortical GABA, striatal dopamine and midbrain serotonin as the key players in compulsive and anxiety disorders - Results from in vivo imaging studies. Rev. Neurosci. 21: 119–139.

Nikolaus, S., Larisch, R., Vosberg, H., Beu, M., Wirrwar, A., Kley, K., Antke, C., De Souza-Silva, M.A., Huston, J.P. and Müller, H.W. (2011). Pharmacological challenge and synaptic response – assessing dopaminergic function in the rat striatum with small animal SPECT and PET. Rev. Neurosci. 22: 625–645.

Nikolaus, S., Hautzel, H., Heinzel, A. and Müller, H.W. (2012). Key players in major and bipolar depression – A retrospective analysis of in vivo imaging studies. Behav. Brain Res. 232: 358–390.

Nikolaus, S., Hautzel, H. and Müller, H.W. (2014a). Neurochemical dysfunction in treated and nontreated schizophrenia – a retrospective analysis of in vivo imaging studies. Rev. Neurosci. 25: 25–96.

Nikolaus, S., Hautzel, H. and Müller, H.W. (2014b). Focus on $GABA_A$ receptor function – a comparative analysis of in vivo imaging studies on neuropsychiatric disorders. Nuklearmedizin 53: 227–237.

Nikolaus, S., Beu, M., de Souza Silva, M.A., Huston, J.P., Antke, C., Müller, H.W. and Hautzel, H. (2017). GABAergic control of neostriatal dopamine D2 receptor binding and behaviors in the rat. Pharmacol. Biochem. Behav. 153: 76–87.

Nikolaus, S., Wittsack, J., Beu, M., De Souza Silva, M.A., Huston, J.P., Müller-Lutz, A., Wickrath, F., Antke, C., Antoch, G., Müller, H.W. and Hautzel, H. (2018a). GABAergic control of nigrostriatal and mesolimbic dopamine in the rat brain. Front. Behav. Neurosci. 12: article 38, https://doi.org/10.3389/fnbeh.2018.00038.

Nikolaus, S., Beu, M., Antke, C. and Müller, H.W. (2018b). Translating neurochemistry: benefit of joint behavioral and in vivo imaging studies in the rat for neuropsychiatric disorders. J. Tansl. Sci. 5: 1–3.

Nikolaus, S., Wittsack, J., Wickrath, F., Müller-Lutz, A., Hautzel, H., Beu, M., Antke, C., Mamlins, E., De Souza Silva, M.A., Huston, J.P., Antoch, G. and Müller, H.W. (2019a). D-cycloserine and amantadine exert opposite effects on motor behavior and $D_{2/3}$ receptor binding in the rat nigrostriatal and mesolimbic system. Sci. Rep. 9*:* 16128.

Nikolaus, S., Wittsack, J., Beu, M., Antke, C., Hautzel, H., Wickrath, F., Müller-Lutz, A., De Souza Silva, M.A., Huston, J.P., Antoch, G. and Müller, H.W. (2019b). Amantadine enhances nigrostriatal and mesolimbic dopamine function in the rat brain in relation to motor and exploratory activity. Pharmacol. Biochem. Behav. 179: 156–170.

Oakley, N.R., Hayes, A.G. and Sheehan, M.J. (1991). Effect of typical and atypical neuroleptics on the behavioural consequences of activation by muscimol of mesolimbic and nigro-striatal dopaminergic pathways in the rat. Psychopharmacology (Berl) 105: 204–208.

Onoe, H., Inoue, O., Suzuki, K., Tsukada, H., Itoh, T., Mataga, N. and Watanabe, Y. (1994). Ketamine increases the striatal N-^{11}C-methylspiperone binding in vivo: positron emission tomography study using conscious rhesus monkey. Brain Res. 663: 191–198.

Paxinos, G. and Watson, C. (2014). The rat btain in stereotaxix coordinates. 7th edition. Academic Press, Elesevier, Amsterdam.

Polc, P., Pieri, L., Bonetti, E.P., Scherschlicht, R., Moehler, H., Ketler, R., Burkard, W. and Haefely, W. (1986). L-cycloserine: behaviotal and biochemical effects after single and repeated administration to mice, rats and cats. Neuropharmacology 25: 411–418.

Quack, G., Hesselink, M., Danysz, W. and Spanagel, R. (1995). Microdialysis studies with amantadine and memantine on pharmacokinetics and effects on dopamine turnover. J. Neural Transm. (Suppl.) 46: 97–105.

Saito, H., Matsumoto, M., Togashi, H. and Yoshioka, M. (1996). Functional interaction between serotonin and other neuronal systems: focus on in vivo microdialysis studies. Jpn. J. Pharmacol. 70: 203–205.

Santiago, M. and Westerink, B.H. (1992). The role of GABA receptors in the control of nigrostriatal dopaminergic neurons: dual-probe microdialysis study in awake rats. Eur. J. Pharmacol. 219: 175–181.

Scatton, B., Cheramy, A., Besson, M.J. and Glowinski, J. (1970). Increased synthesis and release of dopamine in the striatum of the rat after amantadine treatment. Eur. J. Pharmacol. 13: 131–133.

Scotto, P., Monaco, P., Scardi, V. and Bonavita, V. (1963). Neurochemical studies with L-cycloserine, a central depressant agent. J. Neurochem. 10: 831–839.

Schiffer, W.K., Mirrione, M.M., Biegon, A., Alexoff, D.L., Patel, V. and Dewey, S.L. (2006). Serial microPET measures of the metabolic reaction to a microdialysis probe implant. J. Neurosci. Methods 155: 272–284.

Schramm, N., Wirrwar, A., Sonnenberg, F. and Halling, H. (2000). Compact high resolution detector for small animal SPECT. IEEE Trans. Nucl. Sci. 47, 1163–1166.

Seeman, P. and Grigoriadis, D. (1987). Dopamine receptors in brain and periphery. Neurochem. Int. 10: 1–25.

Seneca, N., Finnema, S.J., Farde, L., Gulyás, B., Wikström, H.V., Halldin, C. and Innis, R.B. (2006). Effect of amphetamine on dopamine D2 receptor binding in nonhuman primate brain: a comparison of the agonist radioligand [11C]MNPA and antagonist [11C]raclopride. Synapse 59: 260–269.

Smeal, R.M., Gaspar, R.C., Keefe, K.A. and Wilcox, K.S. (2007). A rat brain slice preparation for characterizing both thalamostriatal and corticostriatal afferents. J. Neurosci. Methods 159: 224–235.

Smolders, I., De Klippel, N., Sarre, S., Ebinger, G. and Michotte, Y. (1995). Tonic GABA-ergic modulation of striatal dopamine release studied by in vivo microdialysis in the freely moving rat. Eur. J. Pharmacol. 284: 83–91.

Takahashi, T., Yamashita, H., Zhang, Y.X. and Nakamura, S. (1996). Inhibitory effect of MK-801 on amantadine-induced dopamine release in the rat striatum. Brain Res. Bull. 41: 363–367.

Turner, M.S., Lavin, A., Grace, A.A. and Napier, T.C. (2001). Regulation of limbic information outflow by the subthalamic nucleus: excitatory amino acid projections to the ventral pallidum. J. Neurosci. 21: 2820–2832.

Videbaek, C., Toska, K., Scheideler, M.A., Paulson, O.B. and Moos Knudsen, G. (2000). SPECT tracer [^{123}I]IBZM has similar affinity to dopamine D2 and D3 receptors. Synapse. 38: 338–342.

Volonté, M.A., Moresco, R.M., Gobbo, C., Messa, C., Carpinelli, A., Rizzo, G., Comi, G. and Fazio, F. (2001). A PET study with [^{11}C]raclopride in

Parkinson's disease: preliminary results on the effect of amantadine on the dopaminergic system. Neurol. Sci. 22: 107–108.
Walaas, I. and Fonnum, F. (1980a). Biochemical evidence for glutamate as a transmitter in hippocampal efferents to the basal forebrain and hypothalamus in the rat brain. Neuroscience 5: 1691–1698.
Walaas, I. and Fonnum, F. (1980b). Biochemical evidence for gamma-aminobutyrate containing fibres from the nucleus accumbens to the substantia nigra and ventral tegmental area in the rat. Neuroscience 5: 63–72.
Watabe-Uchida, M., Zhu, L., Ogawa, S.K., Vamanrao, A. and Uchida, N. (2012). Whole-brain mapping of direct inputs to midbrain dopamine neurons. Neuron 74, 858–873.
Westerink, B.H., Santiago, M. and De Vries, J.B. (1992). *In vivo* evidence for a concordant response of terminal and dendritic dopamine release during intranigral infusion of drugs. Naunyn-Schmiedeberg's Arch. Pharmacol. 346: 637–643.
Westerink, B.H., Kwint, H.F. and deVries, J.B. (1996). The pharmacology of mesolimbic dopamine neurons: a dual-probe microdialysis study in the ventral tegmental area and nucleus accumbens of the rat brain. J. Neurosci. 16: 2605–2611.
Westerink, B.H., Enrico, P., Feimann, J. and De Vries, J.B. (1998). The pharmacology of mesocortical dopamine neurons: a dual-probe microdialysis study in the ventral tegmental area and prefrontal cortex of the rat brain. J. Pharmacol. Exp. Ther. 285: 143–154.
Xia, Y.F., Margolis, E.B. and Hjelmstad, G.O. (2010). Substance P inhibits GABAB receptor signalling in the ventral tegmental area. J .Physiol. 588: 1541–1549.
Yan, Q. (1999). Focal bicuculline increases extracellular dopamine concentration in the nucleus accumbens of freely moving rats as measured by in vivo microdialysis. Eur. J. Pharmacol. 385: 7–13.
Yang, E., Ravikumar, P., Allen, G.L., Baker, Y., Wan, Y.W. and Liu, Z. (2014). A general framework for mixed graphical models. arXIV: 1411.0288 [math.ST].
Yousefi, B., Nasehi, M., Khakpai, F. and Zarrindast, M.R. (2012). Possible interaction of cholinergic and GABAergic systems between MS and CA1 upon memory acquisition in rats. Behav. Brain Res. 235: 231–243.
Zhang, S. and Cranney, J. (2008). The role of GABA and anxiety in the reconsolidation of conditioned fear. Behav. Neurosci. 122: 1295–1305.
Zlomuzica, A., De Souza Silva, M.A., Huston, J.P. and Dere, E. (2007). NMDA receptor modulation by D-cycloserine promotes episodic-like memory in mice. Psychopharmacology (Berl) 193: 503–509.